(11) EP 4 407 634 A1

(12)

EUROPEAN PATENT APPLICATION

(43) Date of publication: 31.07.2024 Bulletin 2024/31

(21) Application number: 23305107.7

(22) Date of filing: 27.01.2023

(51) International Patent Classification (IPC): **G21K** 1/00 (2006.01)

(52) Cooperative Patent Classification (CPC): **G21K 1/006**

(84) Designated Contracting States:

AL AT BE BG CH CY CZ DE DK EE ES FI FR GB GR HR HU IE IS IT LI LT LU LV MC ME MK MT NL NO PL PT RO RS SE SI SK SM TR

Designated Extension States:

BA

Designated Validation States:

KH MA MD TN

(71) Applicant: Institut Optique Theorique Appliquee 91127 Palaiseau Cedex (FR)

(72) Inventor: **BERTOLDI, Andrea**33400 TALENCE (FR)

(74) Representative: Atout PI Laplace Immeuble Up On 25 Boulevard Romain Rolland CS 40072 75685 Paris Cedex 14 (FR)

(54) IMPROVED COLD ATOM SOURCE

- (57) The invention concerns a cold atom source (10) comprising:
- a primary atom source (PAS),
- a two-dimensional magneto-optical trap, called 2D-MOT, comprising :
- ❖ a first pair (LB1, LB1') and a second pair (LB2, LB2') of two counterpropagating beams,
- a magnetic device (MD) configured to generate a magnetic field
- a cooling beam (CBm) propagating in a direction oppo-

site to that of the atoms, the cooling beam presenting a frequency detuning with respect to a frequency of a cooling transition having a negative value $\Delta_{\rm Z} m$ depending on the atom species, said frequency detuning being determined so that a first set of atoms presenting speeds comprised in a first speed interval (IS1) at an exit of the atom primary source and a second set of atoms presenting speeds comprised in a second speed interval (IS2) greater than the speeds of the first interval, are decelerated by resonance with respectively a first and a second circular polarization component of the cooling beam.

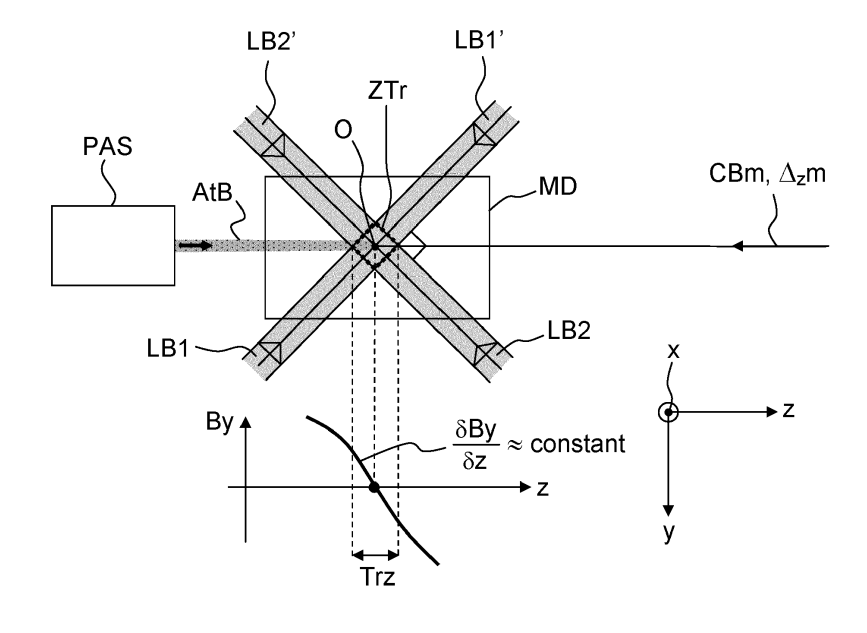


FIG 7

EP 4 407 634 /

Description

BACKGROUND

5 FIELD

15

30

35

45

50

[0001] The invention relates to the field of cold atom source, and more particularly on cold atoms source based on the combination of a two-dimensional magneto-optical-trap, called 2D-MOT, and a Zeeman slower.

10 RELATED ART

[0002] Cold atom sources have been developed for different applications such as atomic clocks, gravimeters, accelerometers, gyroscopes, among others... For the industrialization of those quantum sensors there is presently a need for developing miniaturized cold atoms sources.

[0003] A first cold atom source 20, called Zeeman slower, has been described by Phillips et al in the publication "Laser Deceleration of an Atomic Beam" (Phys.Rev. Lett. Vol 48, n°9, 1982) and is illustrated in figure 1. The Zeeman slower is based on the deceleration of atoms by a counter-propagating laser beam called Zeeman beam ZB. The atoms have a two level atomic structure with a fundamental state FS and an excited state ExS, the transition between the two states being called the cooling transition defined by the transition wavelength λc or the transition frequency f_c . The Zeeman laser has a wavelength related to λc . In order to efficiently decelerate the atoms, the photons of the Zeeman beam need to be in resonance with the atoms.

[0004] The effective atomic deceleration is limited by two processes: the changing atomic velocity Doppler shifts out of resonance of laser light, and optical pumping limits the number of available photon scattering cycles. The atom source of Phillips solves those two problems.

[0005] The cold atoms source 20 comprises a primary atom source PS which is an oven: atoms with a low vapour pressure at 300 K typically require an oven to generate a thermal atomic beam with sufficient flux. This is the case of strontium (Sr), sodium (Na), cadmium (Cd), and ytterbium (Yt) among others. The Phillips source uses Na atoms and the transition between the FS = 3S (F=2, M_F=2) ground state and the ExS = 3P (F=3, M_F=3) excited state. The typical operating temperature of an oven is a few hundred degree Celsius, which determines a Maxwell-Boltzmann distribution for the velocity of the thermal atomic beam AtB generated by the oven, with a root mean square value at a few hundred meters/seconds out of the oven.

[0006] The cold atom source also comprises a slowing laser beam ZB with a fixed frequency and having a circular polarization, generated by a cooling laser CL.

[0007] The Zeeman slower uses a spatially varying magnetic field Bz along the axis z of the thermal atomic beam AtB, and which coincides with the slowing laser beam ZB. The magnetic field Zeeman tunes the decelerating atoms into constant resonance with the fixed-frequency cooling laser CL and produces selection rules and Zeeman shifts that strongly discriminate against optical pumping. The magnetic field keeps the decelerating atoms in resonance with the fixed frequency of the cooling laser thanks to the Zeeman shift, and produces selection rules and Zeeman shifts that strongly inhibit optical pumping. The cold atom source 20 comprises a 60 cm long solenoid SOL configured to generate the spatially varying magnetic field along z Bz

[0008] The spatially-varying magnetic field that optimally compensates the changing Doppler shift of an atom experiencing uniform deceleration a via the constant Zeeman shift γ_Z (expressed in GHz per Gauss) is given by:

$$B=B_b + B_0(1-2az/v_0^2)^{1/2}$$
 (1)

[0009] Where B_b is the constant bias magnetic field which solves the Doppler-shift and pumping problems, and B_0 is the magnetic field for which the Zeeman shift matches the Doppler shift for atoms leaving the oven at an initial velocity v_0 and down to zero velocity.

[0010] Atoms with $v < v_0$ begin decelerating only when they reach the magnetic field which determines a Zeeman shift exactly compensating their Doppler shift. The result is that all atoms with initial velocity up to v_0 are bunched into one slow velocity group, adapt to be trapped.

[0011] Given that the magnetic field is aligned with ZB (along z), the cooling light can be polarized to address only the targeted transition, namely circular positive (negative) if the magnetic sublevel mF increases (decreases) going from FS to ExS. This setup allows an efficient deceleration of atoms but has several drawbacks.

[0012] First, realizing the optimal magnetic field requires a large experimental setup (typically at least 50 cm long, usually 1 m or more depending on the atomic species), a bulky electromagnet configuration which uses high current

and often needs water cooling, or alternatively a complex permanent magnet configuration. This setup cannot be miniaturized

[0013] Second, the atomic trap at the end of the Zeeman slower has the oven in sight, which determines black-body radiation issues and a high collisional rate with background gas which limits the atomic lifetime. To avoid these problems, a mechanical shutter Ch must be installed in vacuum to mechanically hide the path of the thermal atomic beam, or the output atomic beam must be deflected.

[0014] Third, of the atoms leaving the oven, only a small solid angle is captured by the atomic trap, given the long distance required to slow down the thermal atomic beam

[0015] A new configuration introduced by Tiecke et al in the publication "High flux two-dimensional magneto-optical-trap source for cold lithium atoms" (Phys. Rev. A, 80, 013409, 2009) relies on a 2D-MOT transversely loaded with the atomic beam effused by an oven along the z axis.

[0016] The geometrical configuration of the laser beams of the 2D-MOT of Tiecke is shown on figure 2A (perspective), figure 2B (yz plane - 2D-MOT plane), and figures 2C and 2D shows the magnet configuration in the yz plane (magnets plane). Note that in figures 2A to 2D the axis z (propagation of atom beam) corresponds to axis y of Tiecke, and axis x (toward the second chamber) corresponds to axis z of Tiecke.

[0017] The 2D-MOT cools and traps atoms along the *y-z* plane, whereas leaves the *x* free for the transfer of atoms to another chamber (operated by a push beam), where another MOT called 3D-MOT (recapture) is located. The 2D-MOT is the first phase of the cooling process, and the second phase occurs in the second chamber with the 3D-MOT.

[0018] The 2D-MOT comprises 4 counter-propagating laser beams in pairs, a first pair of contra-propagating beams (LB1, LB1') and a second pair of contra-propagating beams (LB2, LB2'), the two pairs (LB1, LB1') and (LB2, LB2') being perpendicular to each other. The beams are located in the y-z plane (2D-MOT plane) at an angle $\pm \pi/4$ with respect to the z axis and red detuned with respect to the cooling transition. The two pairs have opposite circular polarization, and the polarization of the two beams in each pair is also opposite. The zone ZTr at the intersection of the beams defines the trap dimension, having a centre O. In Tiecke atoms are Lithium and the cooling transition is around 671 nm. The four beams for the 2D-MOT (and the 6 beams for the 3D-MOT) are provided by a unique laser system.

[0019] The 2D-MOT also comprises two sets S1t and S2t of stacked permanents magnet configured to generate a two-dimensional magnetic field with:

i) a zero magnetic field at the centre O and along the x axis in the trap zone ZTr, and,

15

30

50

55

ii) a component By along y with a nearly constant gradient VB = δ By/ δ z (monotone variation) around point O in the trap zone ZTr; the constant value may be negative or positive, with an adaptation of the polarizations of all the 2D-MOT beams.

[0020] The two sets are arranged symmetrically with respect to the z axis along y and have equal but opposite magnetization +M/-M along z as shown on figure 2C.

[0021] As the B field is null along the x axis, and along the z axis is aligned on y and has a constant gradient, then the second Maxwell equation (i.e. the Gauss's law of magnetism) imposes that along the y axis the B field is aligned on z and has a gradient opposite to that along the z axis.

[0022] This magnetic field B field being null along one axis (the x one) and varying linearly and with opposite gradient along the two other axes is commonly called linear quadrupole magnetic field.

[0023] Applying an optimized magnetic field as described above is a necessary condition for efficient capture of atoms in the 2D-MOT. The optimal value of the constant gradient G depends on the atom species and is determined analytically (see for example publication Raab et al, Phys.Rev. Lett., vol 59, n°23, p 2631 1987) so as to obtain an overdamped motion for the atoms trapped in the 2D-MOT.

[0024] Note that in a 3D-MOT configuration the B field is null in only one point, has a gradient G_{3D} along one axis and a gradient $-G_{3D}/2$ along the other two axes.

[0025] An atom with a velocity low enough to be captured by the 2D-MOT entering in the region where the 2D-MOT laser beams overlap experiences a combination of friction and central force, which cools the atom and traps it on the x axis. Differently from a 3D MOT, where the force acts along the 3 main axes, in a 2D MOT it acts along 2 axes (y and z) whereas the atoms are free along the third one (x axis).

[0026] This configuration has the advantage of being very compact and strongly reduces the distance between the oven and the atom trapping region, thus increasing the capture solid angle compared to the Phillips configuration. The magnetic field is generated by permanent magnets, which is also more compact than the solenoid of Phillips, has a lower consumption and does not need water cooling.

[0027] The 2D MOT produces a jet of cold atoms transferred to another vacuum chamber, where the atoms are recollected (typically in a 3D MOT) and used for the experiment. The place where the atoms are recollected is along the x axis, where the B field generated by the permanent magnet of the 2D MOT is zero. Hence, the magnet configuration

of the 2D MOT does not disturb the final experiment.

10

15

20

30

35

50

[0028] The drawback is that the flux of cold atoms captured by the 2D-MOT in the configuration reported by Tiecke is low when compared to a standard Zeeman slower.

[0029] In two publications, respectively Lamporesi et al (Review of scientific Instruments 84, 063102, 2013) and Nosske et al (Physical. Review A, 96, 053415, 2017) improved the atomic flux reported by Tiecke. Lamporesi realised a sodium source and Nosske a strontium source. In both setups the tail of the 2D MOT magnetic field is exploited to implement a compact non optimized Zeeman slower, which uses a cooling laser beam CB entering the setup along the z axis in the opposite direction with respect to the thermal beam AtB. The Zeeman slower is non optimized because:

i) the magnetic field along the propagation direction of the atomic beam is orthogonal, not parallel, with respect to the Zeeman slower beam and its dependence on z does not respect formula 1,

ii) only half of the Zeeman beam optical power is used to cool the atomic beam, given the detuning adopted for CB and the setup configuration. The polarization of CB is set to be linear along x, which for a magnetic field oriented on y determines an equal contribution of positive and negative circular polarization in the reference frame of the atom. Adopting a linear polarization along y for the CB will result in a π polarization for the atom, which will make the Zeeman shift constant along the z axis, hence no possibility to compensate with the changing Doppler shift of a decelerating atom.

[0030] The geometrical configuration of the 2D MOT of the atom source is the one shown in figures 2A to 2D with a different arrangement of the magnets (four stacks of magnet instead of two). The complete setup of the cold atom source 30 performed by Nosske is shown on figure 3.

[0031] The thermal atom beam AtB is generated by the strontium oven OV operated at a temperature range between 450° to 580°C in the case of strontium. The different beams are included in high vacuum tubes, the trapped atoms are located in the centre of the multiway cross vacuum chamber. The intersection between the 4 2D-MOT beams defines the trap size defined by the zone ZTr. The passage of the trapped atoms from the trap chamber toward the ultra-high vacuum chamber of the 3D-MOT is performed by a differential pumping tube DPT along x, and by a pushing beam PB. The beam AtBC is the cooled atom beam pushed in the 3D-MOT chamber.

[0032] In the two publications the required 2D axial symmetric (along z) linear (because the 0 magnetic field is along one line, axis x) quadrupolar magnetic field is produced by 4 sets S1 to S4, each set having 9 permanent single piece magnets.

[0033] Starting from Tiecke, an equivalent configuration to get the same magnetic field is to rotate the two sets and their magnetization direction in order to put them along the z axis as shown on figure 4.

[0034] But this configuration is impossible as the magnets block the atomic beam. Thus each of the two sets of Tiecke have been "split" in two, and each half has been translated to respectively \pm - x0 as shown on figure 5 (left xz plane, right yz plane). The magnetization axis of S1 and S2 is opposite to the magnetisation axis of S3 and S4. The sets are disposed symmetrically around the chamber at the corners of a rectangle R in the xz plane, centered with respect to the x and z axis with a distance x0 = \pm - 75 mm and z0 = \pm - 88 mm in the x and z direction.

[0035] With this configuration the permanent magnets generate a linear quadrupole magnetic field for the 2D-MOT with a gradient of ~50 G/cm near the origin O where the field is equal to 0.

[0036] The magnetic field By(z) generated by the magnet configuration along the z direction is reported on figure 6. [0037] In addition of serving for the 2D-MOT, the magnetic field is used for an auxiliary Zeeman slower; however, given that the magnetic field is orthogonal to the direction of AtB and ZC, both Lamporesi et al. (end of § II.C in the publication) and Nosske et al. (end of § II.A in the publication) observed that at maximum half the optical power of the Zeeman slower beam can be set on each of the two polarizations in the atom reference system, and hence used for the atom deceleration. This configuration is set by choosing for the Zeeman slower beam a linear polarization along the axis orthogonal to the magnetic field, i.e. x for Nosske and y for Lamporesi. By choosing a linear polarization along the axis of the magnetic field, i.e. along y for Nosske and x for Lamporesi only π transitions are induced on the atoms, and no Zeeman deceleration is feasible because the ground and excited levels of the addressed transition are shifted in the same way by the magnetic field.

[0038] The cooling beam of the Zeeman slower and the 2D-MOT beams have frequency offset equal to several natural linewidth Γ (linewidth of the two hyperfine levels of the atomic structure, specific to each atom species).

[0039] In the Nosske setup of figure 6 the centre of the trap is located at 125 mm from the exit of the oven (strontium source). The size of the ZTr zone along the y axis Try is +/- 15 mm.

[0040] The cooling transition of strontium is between the fundamental state FS = $5s^2 \, ^1S_0$ and the excited state ExS = $5s5p \, ^1P_1$, corresponding to a wavelength $\lambda c = 461$ nm.

[0041] On figure 6 Nosske defines two regions of the magnetic field topology allowing for the Zeeman slower, labelled 1 and 2 on figure 4. In region 1 the magnetic field increases until a maximum value Bmax of 160 G and the gradient is

positive, in region 2 the magnetic field decreases from Bmax, passes at zero value at the centre O of the trap and continues to decrease until a minimum value -Bmax, and the gradient is negative.

[0042] Publication Nosske considers two possibilities, i.e. using region 1 or region 2 exploiting one polarization component of the cooling beam or the other. The magnetic field gradient reaches a maximum of about 15 G/cm in region 1 and about twice as large (30 G/cm) in region 2. Nosske finds that region 2 is more efficient than region 1 for the Zeeman slowing, and supposes that this is due to a lower impact of collisions with hot atoms (see § V of the publication). For strontium $\Gamma/2\pi = 32$ MHz and the optimal offset of the cooling beam $\Delta_z(N)$ is equal to -210 MHz (= -6.6. $\Gamma/2\pi$) (table I if the publication).

[0043] The Lamporesi publication assumes that the cooling of the thermal beam is operated on « the vanishing tail » of the magnetic field generated by the permanent magnets , i.e. the region from the oven to the position where the magnetic field is maximum, corresponding to region 1 of Nosske. The gradient around the centre is 0.36 T/m (corresponding to 36 G/cm). For sodium $\Gamma/2.\pi$ = 9.79 MHz, and in Lamporesi the offset of the cooling beam $\Delta z(L)$ is equal to -304 MHz (= -31. $\Gamma/2\pi$) (table I if the publication).

[0044] In the two publications the optimal detuning of the Zeeman slower beam CB, $\Delta_z(L)$ and $\Delta_z(N)$, is determined experimentally without a physical explanation/comprehension on the effect of the detuning value.

[0045] Both Lamporesi and Nosske state that at maximum half of the optical power of the cooling beam can be exploited to slow down the thermal atomic beam. The cooling beam is linearly polarized along the zero magnetic field axis of the 2D-MOT and can be decomposed in two circular components σ^+ and σ^- . Exploiting half of the available optical power means that only one circular component decelerates the atoms, and the other one is wasted.

[0046] The target of the invention is to realize an atomic source which combines compactness and low energy consumption with a high flux of cold atoms. The design of the cold atom source according to the invention has a geometry close to the one described in Lamporesi/Nosske, but the frequency detuning of the cooling beam, and optionally magnetic field parameters, are modified in order to achieve a larger cold atomic flux.

SUMMARY OF THE INVENTION

10

15

20

25

35

40

45

50

[0047] There is provided a cold atom source comprising:

- a primary atom source configured to generated an atomic beam propagating along a z direction of a coordinate system xyz,
 - a two-dimensional magneto-optical trap, called 2D-MOT, comprising:
 - a first pair and a second pair of two counter-propagating beams, the two pairs being perpendicular to each other and located in a plane yz, the intersection of which defining a trap zone having a centre O,
 - a magnetic device configured to generate a magnetic field having :
 - ❖ a null value at centre O and on the x axis at least inside the trap zone,
 - ❖ a component along y By having a gradient along the z axis being almost constant in the trap zone, an absolute value of said constant depending on the atom species,
 - ❖ the component along y By varying along the z axis between two extrema, a positive maximum and a negative minimum, said positive maximum and said negative minimum having identical absolute values,
 - a cooling beam propagating in a direction opposite to that of the atoms, the cooling beam presenting a frequency detuning with respect to a frequency of a cooling transition having a negative value Δ_zm depending on the atom species, said frequency detuning being determined so that a first set of atoms presenting speeds comprised in a first speed interval at an exit of the atom primary source and a second set of atoms presenting speeds comprised in a second speed interval (IS2) greater than the speeds of the first interval, are decelerated by resonance with respectively a first and a second circular polarization component of the cooling beam, the second speed interval being contiguous to the first speed interval.
- [0048] According to a development the magnetic device comprises two sets of stacked permanent magnets, respectively arranged along the y axis symmetrically on either side of the z axis and having respective magnetic dipoles oppositely oriented along the z axis.

[0049] According to a development the magnetic device comprises four sets of stacked permanent magnets, arranged

at the corners of a rectangle in the xz plane centred in O, the two sets arranged on the primary source side and the two sets arranged on the other side having respective magnetic dipoles oppositely oriented along the y axis.

[0050] There is provided a cold atom source comprising:

- a primary atom source configured to generated an atomic beam propagating along a z direction of a coordinate system xyz,
 - a two-dimensional magneto-optical trap, called 2D-MOT, comprising :
- a first pair and a second pair of two counter-propagating beams, the two pairs being perpendicular to each other and located in a plane yz, the intersection of which defining a trap zone having a centre O,
 - a magnetic device configured to generate a magnetic field having :

15

20

25

40

50

55

- ❖ a null value at centre O and on the x axis at least inside the trap zone,
- ❖ a component along y By having a gradient along the z axis being constant in the trap zone, an absolute value of said constant depending on the atom species,
- the component along y By varying along the z axis between two extrema, a positive maximum and a negative minimum, an absolute value of the extremum located on a side opposite to the primary atom source being strictly greater than an absolute value of the other extremum,
- a cooling beam propagating in a direction opposite to that of the atoms, the cooling beam presenting a frequency detuning Δ_z m with respect to a frequency of a cooling transition having a negative value depending on the atom species.

[0051] According to a development the absolute value of the extremum located on the side opposite to the primary atom source is strictly greater than the absolute value of the other extremum, of a factor (K) being comprised between 1.3 and 3.

- [0052] According to a development the magnetic device comprises four sets of stacked permanent magnets arranged at the corners of a rectangle in the xz plane centred in a point O' located on the z axis but offset from O, the two sets arranged on the primary source side and the two sets arranged on the other side having respective magnetic dipoles oppositely oriented along the y axis, and an absolute value of the magnetic dipoles of the two sets arranged on the primary source side being smaller than an absolute value (M1) of the two sets arranged on the other side.
- [0053] According to a development the cooling beam presents an additional frequency detuning Δ_z m' determined from the frequency detuning Δ_z m by the formula :

$$\Delta_z$$
m' = Δ_z m - 2 μ_B B_{PSS} / \hbar - 2 Γ /(2 π) +/- 2 Γ /(2 π)

with μ_B the Bohr magneton, \hbar the Planck constant and $\Gamma/(2\pi)$ the natural linewidth of the atom species, and B_{PSS} is the absolute value of the magnetic field extremum located on the primary atom source side.

[0054] According to a development the atom species is chosen among: Strontium; Ytterbium; Calcium; Magnesium; Cadmium; Sodium.

[0055] According to a development the frequency detuning Δ_7 m is such that:

$$-1500 \text{ MHz} \le \Delta_z \text{m} \le -325 \text{ MHz}$$

[0056] According to a development the primary atom source is an oven.

[0057] Alternatively according to development the primary atom source is a solid atomic source whose desorption is controlled by a laser source.

BRIEF DESCRIPTION OF THE DRAWINGS

[0058] Embodiments of the present invention, and further objectives of advantages thereof, are described in details

below with reference to the attached figures, wherein:

5

10

15

20

30

35

40

45

50

Ciaura 1	l alraadu	aucted	doooribooo	aald atam	aguraa baaad	an a 7aaman	alaurar aga	ardina ta	the etete	of the ort
ridure	ı aireauv	auotea	describes a	colo alom	source based	on a zeeman	Slower acc	oraina to	the state	oi ine ari

- Figure 2A already quoted describes the geometry in perspective view of the four beams of two-dimensional magneto optical trap, called MOT 2D, according to the state of the art.
 - Figure 2B already quoted describes the geometry in the yz plane of the four beams of the two-dimensional magneto optical trap called MOT 2D according to the state of the art.

Figure 2C already quoted describes a first geometry of the magnets in the yz plane of state of the art.

Figure 2D already quoted shows the magnetic field variation necessary for the trapping of the atom in a MOT-2D according to the state of the art.

Figure 3 already quoted describes an improved 2D-MOT configuration comprising a Zeeman slower beam according to the state of the art.

Figure 4 already quoted describes another magnet geometry impossible to implement.

Figure 5 describes a second magnet geometry of the state of the art.

Figure 6 shows the variation of the component By as a function of z according to the state of the art.

Figure 7 shows the basic principle of the cold atom source according to the invention.

Figure 8 shows an example of the cold atom source according to the first variant of the invention.

Figure 9 shows an example of the phase-space plot of the different atomic velocities effused by the oven, for a 2D-MOT alone according to the state of the art.

Figure 10 shows the corresponding Maxwell-Boltzmann distribution of the velocity of the atoms emitted by the oven (dark grey), and after the action of the trap is taken into account (light grey), for the 2D-MOT alone according to the state of the art.

Figure 11 shows the phase-space plot of the different atomic velocities in the presence of a cooling beam with a nominal detuning equal to -210 MHz for strontium and according to the state of the art.

Figure 12 shows the velocities distribution corresponding to the case of figure 11.

Figure 13 shows a phase-space plot with the atomic trajectories for the atoms effused by the oven modified by the combined effect of the magnetic field and the cooling beam opposite to the atomic beam and with a detuning Δ_z with respect to the cooling transition, for the first variant of the invention and neglecting the off-resonance scattering of photons.

Figure 14 shows the atom trajectories in the phase space corresponding to an optimal set of parameters and according to the first variant of the invention.

Figure 15 shows the corresponding Maxwell-Boltzmann distribution of the velocity of the atoms emitted by the oven (dark grey), and after the action of the trap is taken into account (light grey), for the same set of parameters as in figure 14, according to the first variant of the invention.

Figure 16 shows an example of a cold atom source according to the second variant of the invention.

Figure 17 shows a phase-space plot with the atomic trajectories for the atoms effused by the oven modified by the combined effect of the magnetic field and the cooling beam opposite to the atomic beam and with a detuning Δ_z with respect to the cooling transition, for the second variant of the invention.

Figure 18 shows the atom trajectories in the phase space corresponding to an optimal set of parameters and according to the second variant of the invention.

Figure 19 shows the corresponding Maxwell-Boltzmann distribution of the velocity of the atoms emitted by the oven (dark grey), and after the action of the trap is taken into account (light grey), for the same set of parameters than for figure 18, according to the second variant of the invention.

Figure 20 shows a phase-space plot with the atomic trajectories for the atoms according to an embodiment of the invention, in combination of the second variant of the invention, where the cooling beam presents an initial detuning Δ_7 with respect to the cooling transition, and an additional detuning Δ_7 correctly chosen.

Figure 21 shows the calculated trajectories in the phase space corresponding to the embodiment of the invention where the cooling beam presents an initial detuning Δ_z with respect to the cooling transition, and an additional detuning Δ_z ' correctly chosen, for the second variant of the invention.

Figure 22 shows the corresponding Maxwell-Boltzmann distribution of the velocity of the atoms emitted by the oven (dark grey), and after the action of the trap is taken into account (light grey), for the same set of parameters as in figure 21, according to the second variant of the invention.

DETAILED DESCRIPTION OF THE INVENTION

5

10

15

20

30

35

45

50

55

[0059] Starting from the Lamporesi/Nosske configuration, the inventor approach consists in understanding in detail the physical effects involved in this trap combining 2D-MOT and non-optimized Zeeman slower, in order to improve its performance by modifying parameters of interest.

[0060] The numerical simulation used in Lamporesi considers separately the atomic dynamics from the oven until the the 2D MOT region and inside the 2D MOT, and did not identify the peculiar features of the atomic trajectories (e.g. that atoms can be captured by the 2D-MOT in their second passage in the trapping region), trap operation and efficiency (e.g that both polarization components of the Zeeman cooling beam can be used simultaneously for the atom deceleration).

[0061] The cold atom source 10, 11 according to the invention is shown on figure 7. The cold atom source comprises a primary atom source PAS configured to generate an atomic beam AtB propagating along a z axis of a coordinate system xvz.

[0062] According to one embodiment the primary source is an oven. The output of the oven can be a single aperture or it can be filled with an array of micro-tubes to increase the source collimation.

[0063] According to another embodiment the primary source is a solid atomic source, whose desorption is controlled by a laser source, as reported in Kock et al in "Laser controlled atom source for optical clocks" Scientific Reports 6, 37321 (2016) where a thermal jet of atoms is obtained by laser ablation with a laser source preferentially in the ultraviolet range.

[0064] The cold atom source also comprises a two-dimensional magneto-optical trap, called 2D-MOT, comprising a first pair (LB1, LB1') and a second pair (LB2, LB2') of two counter-propagating beams. The two pairs are perpendicular to each other and located in a plane yz, and the intersection of which defines a trap zone ZTr having a centre O. The dimension of the trap along the z axis is Trz. The four beams LB1, LB1', LB2, LB2' trap and cool the atoms and the configuration of the four beams is identical to that of Lamporesi/Nosske.

[0065] The 2D-MOT also comprises a magnetic device MD configured to generate a magnetic field having a null value at centre O and on the x axis at least inside the trap zone. Moreover the component of the magnetic field B along y By has a gradient along the z axis almost constant in the trap zone, and the value of the constant depends on the atom species:

$\nabla B = \delta B y / \delta z \cong constant$

[0066] In Nosske, Lamporesi and figure 7 the value of the magnetic field gradient is negative. According to another embodiment the gradient is positive, which requires the inversion of the polarization of the 2D MOT beams, and the exchange of the role of each polarization component in the Zeeman slower.

[0067] The cold atomic source 10, 11 also comprises a cooling beam CBm propagating in a direction opposite to that of the atoms. The cooling beam CBm has a linear polarization along the x axis, which is decomposed into a balanced sum of right circular polarisation σ^+ component and a left circular polarization σ^- component. Note that a circular polarization along the y axis would determine only π transitions on the atoms, which are useless in a Zeeman slower.

[0068] The cooling beam is generated by a laser not shown on figure 7. The cooling beam CBm has a frequency fcb which is detuned from the frequency fc of the cooling transition of the atom species of the beam AtB, of a negative value $\Delta_z m$:

 $fcb = fc - |\Delta_z m| \qquad (1)$

[0069] Values of the detuning Δ_z m as claimed, different from those of the state of the art, are discussed further. As will be shown later a detuning as claimed Δ_z m allows the use of both polarizations σ^+ and σ^- for the cooling of the atoms, resulting in a greater flux of trapped atoms.

[0070] All the beams are located in interconnected vacuum chambers.

5

10

30

50

55

[0071] An example of the cold atom source 10 according to the first variant of the invention is shown on figure 8, based on the Nosske configuration. The trap configuration is shown on A, the applied magnetic field By is plotted on B and the configuration of the four magnet sets in the xz plane is shown on C.

[0072] In the cold atom source 10 according to the first variant the magnetic device MD is configured so that the component along y By varying along z between two extrema, a positive maximum and a negative minimum as shown on figure 8 B. In the first variant the positive maximum value Bmax and the negative minimum value Bmin have identical absolute values: |Bmin| = Bmax.

[0073] In order to have a zero value of By at O the two extrema are symmetrically arranged with respect to the centre O. [0074] Note that with a positive gradient value the respective position of the maximum and minimum of the magnetic field By are reversed.

[0075] According to one embodiment magnetic device MD comprises two sets (S1t, S2t) of stacked permanent magnets, respectively arranged symmetrically on either side the z axis and having respective magnetic dipoles oppositely oriented along the y axis, as illustrated on figure 2C.

[0076] According to another embodiment the magnetic device MD comprises four sets of stacked permanent magnets, arranged at the corners of a rectangle R in the xz plane centred in O. The two sets (S3, S4) arranged on the primary source side and the two sets (S1, S2) arranged on the other side have respective magnetic dipoles \vec{M} oppositely oriented along the y axis, as shown on figure 8 C (similarly to Nosske magnets configuration shown on figure 5).

[0077] In this non-limiting example the primary source is an oven of strontium located at z=-15 cm from the centre O. The size of the trap (overlapping of the 4 MOT beams) along z is Trz = +/-2 cm. A sapphire viewport SW located at z=+35 cm allows to send the laser light of the Zeeman laser in the direction of the oven and in opposite direction with respect to the thermal atomic beam it produces. The viewport is heated to avoid its rapid metallization caused by the strontium thermal beam, for example for strontium to ~ 300 °C.

³⁵ **[0078]** The distance d_{ps-O} between the primary source and the trap centre O sizes the atom source taking into account the many design and physical constraints. We want this distance as short as possible but it cannot currently be less than 10 cm. A distance of 15 cm is currently a standard for cold atom sources design.

[0079] The maximum B_{max} (minimun B_{min}) of the magnetic field on the z axis at the position of the magnet stacks is set by the magnet configuration (i.e. position of the magnets and required gradient VB).

[0080] For strontium with a negative gradient VB= δ By/ δ z= -Gr ~- 40 G/cm, B_{max} ~ 160 G at -z0 = -5 cm and Bmin ~ -160 G at z0 = +5 cm (see figure 8 B).

[0081] On figure 8 (A) the two regions 1 and 2 already identified by Nosske are shown and also two additional regions 3 and 4. Region 3 starts from the centre O and ends at the minimum +z0 of the magnetic field and region 4 starts at the end of region 3 and finishes at the sapphire window at z=35cm.

[0082] To better understand the atomic dynamics along z before the trap and in the trap until O (regions 1 and 2), but also in the regions 3 and 4 located after the centre O, the inventors have developed a numerical simulation which calculates the atoms trajectories from the oven and until the trajectories ends up. The simulation uses the 4th order Runge-Kutta algorithm to calculate the atomic dynamics in the presence of i) magnetic field generated by the four stacks of permanent magnets, and ii) of the laser beams of the 2D-MOT and iii) the Zeeman cooler beam. The simulation is based on the configuration of figure 8 (A).

[0083] A first simulation takes into account the 2D-MOT alone without Zeeman cooling beam, with an applied magnetic field as in figure 8 (B) with magnets as in figure 8 (C). Figure 9 shows the phase-space plot of the different atomic velocities effused by the oven. It shows trajectories of the atoms along z as a function of the initial speed along z vz at the exit of the oven at 585°C. The white lines/curves correspond to trajectories which are not trapped in the 2D-MOT and the black lines the trajectories which are trapped by the 2D-MOT in the origin.

[0084] The background colour corresponds to the value of the acceleration a_{MAX} of the atoms: grey: no acceleration; white: negative acceleration; black: positive acceleration. The atoms are decelerated because they diffracts photons and the amount of photons they can diffract depends on the atom species and more particularly on the natural linewidth

 Γ and on the intensity and frequency of the laser light. The maximum acceleration a_{MAX} is given by the formula :

 $a_{\text{max}} = \hbar k/2M\tau$ (2)

15

20

25

35

50

where k is the wavenumber associated with the cooling beam, \hbar the reduced Planck constant, M the atomic mass and $\tau = 2\pi/\Gamma$ is the lifetime of the excited state of the addressed atomic transition (the cooling transition).

[0085] The acceleration is a vector quantity, whose direction is defined by k; for the Zeeman cooling beam it is directed towards the oven, i.e. against the propagation direction of the atoms effused by the oven. The maximum value of the acceleration is achieved when the laser beam is set to be resonant with the cooling transition and with an intensity much higher than the saturation intensity lsat, which is defined as the intensity required to reduce the absorption coefficient of the atomic medium to half its value.

[0086] The Zeeman cooling beam is not present, so the trajectories are modified only in the 2D-MOT region, because of the acceleration due to the 2D-MOT beams, which determine a friction force slowing the atomic motion together with a central force bringing them towards the x axis.

[0087] The simulation only takes into account the one dimensional propagation along z of the atoms, and does not consider at first the radial expansion of the thermal beam. It can be seen that only the atoms having initial speed positive and below 70 m/s are trapped.

[0088] Figure 10 shows the Maxwell-Boltzmann distribution of the velocities of atoms emitted by the oven (dark grey), almost completely covered by the modified distribution except at low velocity), and after the action of the trap is taken into account (light grey). Only small speeds in the range [0, 70] m/s are captured (left side of the distribution) which corresponds to a very low number of atoms. The peak at 0 velocity 90 represents the atomic fraction captured by the 2D MOT, equal to 0.45%.

[0089] Atoms reaching the HV chamber surfaces 80 of the chamber at a radius r=19 mm thermalize with it, and are lost for the cooling and trapping process. The capture efficiency is corrected to take into account the radial expansion of the atoms during their motion, computed following Greenland et al, Journal of Physics D: Applied Physics 18, 1223 (1985), "Atomic beam velocity distributions". When the losses due to the radial expansion of the thermal beam are taken into account, such capture efficiency decreases to 0.25%.

[0090] Figure 11 shows the phase-space plot of the different atomic velocities in the presence of a cooling beam with a nominal detuning equal to $\Delta_z(N) = -210$ MHz (equal to -6.6 $\Gamma/(2\pi)$ for strontium), which is the best configuration defined in Nosske et al. The background colour indicates the acceleration experienced by the atoms at each position and velocity: in addition to the acceleration due to the 2D MOT, there is now also that determined by the Zeeman cooling beam, always directed towards the oven (hence white coloured). The velocities in resonance with the σ + polarization component of the Zeeman beam along z replicate in the phase plot the shape of the magnetic field, whereas those in resonance with the σ - polarization component of the Zeeman beam z replicate the opposite shape of the magnetic field. The two shapes overlap at z=0, where the magnetic field is null, at a velocity set by the detuning of the Zeeman beam.

[0091] Compared to the configuration where only the 2D-MOT is operated, this one captures atoms in an initial velocity window of similar size, but at higher speed, where the Maxwell-Boltzmann distribution is higher; as a consequence, its capture efficiency results higher, as shown in figure 12.

[0092] Figure 12 shows how the velocity distribution is modified by this experimental configuration. A larger fraction of the Maxwell-Boltzmann initial velocity distribution ends up now in the peak at 0 velocity: 9.2% (peak 120) which is reduced to 4.1 % when radial losses are taken into account.

[0093] It can be seen on figure 11 that only atoms with initial speeds at 170 m/s are trapped in the 2D-MOT "directly", i.e. being decelerated in regions 1 or 2 as reported in Nosske, and thanks to the interaction with the σ + polarization component of the Zeeman beam.

[0094] Atoms with lower speed (see speed interval 103) cannot be trapped as they are decelerated to the inversion point before entering in the 2D-MOT.

[0095] Atoms with initial velocity between 180 m/s and 220 m/s are decelerated in regions 2 and 3, again interacting with the σ + polarization component of the Zeeman beam, to end up trapped after passing beyond the origin; the exploitation of region 3 has never been reported/recognized before, and it is one of the results of the numerical simulation (trajectory 101 on figure 11).

[0096] Atoms with initial speeds ~230-240 m/s pass through the 2D-MOT almost unaffected, and are decelerated along the magnetic field slope in region 4 by the σ -polarization component of the Zeeman beam, and are finally captured by the 2D MOT after their motion is inverted thanks to off-resonance scattering caused by the Zeeman beam (trajectory 102 on figure 11). The exploitation of region 4 has never been reported before, and it is one of the results of the numerical simulation.

[0097] Now it is explained how an optimum range of detuning Δ_z m of the cooling beam can be determined for the first variant of the invention, in order to use both polarization components σ^+ and σ^- of the cooling beam CBm. [0098] The effective detuning Δ_{eff} as seen by an atom at velocity v_z and at a position where the magnetic field is $B_y(z)$ is equal to :

5

$$\Delta_{\text{eff}} = \Delta_{Z-} k v_z + (\mu_B g_F m_F B_v(z)) / \hbar \qquad (3)$$

10 where:

- $k=2\pi/\lambda c$ is the wavenumber associated with the cooling beam, λc the transition wavelength,
- μ_B the Bohr magneton,

15

- g_F the Landé factor,
- \hbar the reduced Planck constant,

20 -

- Δ₇ is the nominal detuning with respect to the resonance condition,
- -kv_z is the Doppler shift determined by the atom velocity v_z and
- + $\mu_B g_F m_F B_v(z)$)/ \hbar is the Zeeman shift of each sublevel m_F determined by the local magnetic field $B_v(z)$.

25

30

35

40

50

55

[0099] The two terms added to the nominal laser detuning are thus the Doppler shift and the Zeeman shift of each sublevel $m_{\rm F}$.

[0100] Figure 13 shows a phase-space plot with the atomic trajectories for the atoms effused by the oven at z=-15 modified by the combined effect of the magnetic field generating the linear quadrupole for the 2D-MOT along the y axis at z=0, and the Zeeman slowing beam CBm opposite to the atomic beam and with a detuning Δ_z with respect to the cooling transition, for the first variant of the invention.

[0101] In order to be captured by the 2D-MOT, the atoms have to enter in the overlap region defined by the MOT beams (-2.0 cm < z < 2.0 cm in the case we consider) with an absolute velocity below the value vc that the 2D MOT can capture. The grey zone CR shows the 2D-MOT capture region, defined by the size of the MOT beams and by the MOT velocity capture v_c . For strontium and parameters of the 2D-MOT of the example, the velocity capture is vc= 70 m/s.

[0102] The magnetic field generated by the permanent magnets for the 2D-MOT has two slopes that can be exploited for the cooling of the thermal beam produced by the oven, when using an opposite circular polarization for the light shined on the opposite direction with respect to the atomic beam, as indicated in figure 13; the first magnetic field slope is in region 1 of figure 13, the second slope in regions 2 and 3 of the same figure.

[0103] It is recalled that for strontium, particularly ⁸⁸Sr (most abundant isotope), the cooling transition is the ¹S₀ - ¹P₁ at 461 nm, with linewidth $\Gamma = 2\pi \times 30.5$ MHz and a saturation intensity I_{sat} = 42.5 mW/cm².

[0104] It is also recalled that the gradient of the magnetic field VB at z=0 is set by the atomic species as a requirement to realize the 2D MOT (for strontium it is ~40 G/cm). The maximum B_{max} of the magnetic on the z axis at the position of the magnet stacks close to the oven is set by the magnet configuration (i.e. position of the magnets and required VB); for strontium and VB-40 G/cm, $B_{max} \sim 160$ G at z=-z0=-5 cm. The minimun B_{min} on the z axis at the position of the magnet stacks far from the oven is the opposite of Bmax and is thus equal to $B_{min} \sim -160$ G at z=z0=5 cm (see figure 8 B and C).

[0105] In figure 13 for simplicity only action of the cooling beam is considered, and the locus of points where it is resonant with the atomic beam is shown with a dashed (dotted) curve for its σ +(σ -) polarization; the off-resonance scattering caused by the Zeeman beam and the presence of the 2D-MOT beams are neglected. The atom velocity window effectively cooled and the final velocity at which the atoms are bunched is determined by the detuning Δz of the cooling beam and by the magnetic field configuration.

[0106] Curve 5 shows in the phase space the atoms being in resonance with the σ^+ polarization component of the cooling beam (detuning Δ_z), and curve 6 shows in the phase space the atoms being in resonance with the σ^- polarization component of the cooling beam. Zone 8 shows the atoms emitted by the oven with a speed (at the exist of the oven) comprised in a first interval IS1 that makes them enter in resonance with the σ^- Zeeman beam component in region 1, and there be decelerated until z=-z0= -5cm. Zone 9 shows the atoms emitted by the oven with a speed comprised in a second interval IS2 that makes them enter in resonance with σ^+ Zeeman beam component in region 2, to be there and

in region 3 decelerated until z= z0 =5 cm.

10

15

35

40

50

55

[0107] A Zeeman cooling beam at a detuning Δ_z is resonant with atoms moving along the z axis at velocity $-\Delta z/k$ wherever the B field is null, condition verified at z=0 (i.e. the 2D MOT position), and well approximated far from the magnet configuration (i.e. at the oven and where the cooling beam enters the setup).

- **[0108]** Elsewhere the cooling beam is resonant with a velocity that depends on the local magnetic field, which shifts the atomic levels. More precisely, it is resonant with:
 - velocities from $-\Delta_z/k + \mu_B B_{min}/(\hbar k)$ to $-\Delta_z/k$ in region 1 via its σ polarization component (atoms of zone 8; 80 m/s to 180 m/s). Note that Δ_z is negative.
 - velocities from $-\Delta_z/k$ to $-\Delta_z/k + \mu_B B_{min}/(\hbar k)$ in region 2 via its σ^+ polarization component (atoms of zone 9 ; 181 m/s to 280 m/s).

[0109] The two groups of atoms cooled by the opposite polarizations are bunched in velocity at the end of the respective slope:

- the atoms cooled in region 1 are at -z0=-5 cm (position of the magnet stacks close to the oven) with v= $-\Delta_z/k + \mu_B$ $B_{min}/(\hbar k)$,
- the atoms cooled in region 2 and 3 are at z=z0= 5cm (position of the magnet stacks far from the oven) have the same speed : $v = -\Delta_z/k + \mu_B B_{min}/(\hbar k)$.

[0110] The effect of the off-resonant photon scattering, neglected in figure 13, is an additional acceleration of the atoms in the -z direction, which lowers the velocity obtained with the Zeeman cooling process and eventually inverts the atomic motion. This effect is taken into account in the simulation of the atomic trajectories to determine if they end up trapped by the 2D-MOT when operative.

[0111] In order for the 2D-MOT to capture atoms decelerated along both magnetic field slopes, the atoms must enter in the 2D-MOT region with a velocity lower in modulus to the capture velocity v_c of the MOT (~70 m/s for Sr and with the MOT beam parameters adopted in the example).

[0112] The velocity of the atoms cooled in region 1 must be reduced by off-resonance scattering of the Zeeman cooling beam from $v = -\Delta_z/k + \mu_B B_{min}/(\hbar k)$ at z = -5 cm to be between 0 m/s and v_c at the negative input of the 2D MOT.

[0113] The trajectory of the atoms cooled in regions 2 and 3 and having a velocity $v = -\Delta_z/k + \mu_B B_{min}/(\hbar k)$ at z=5 cm must be first inverted in region 4 by off-resonance scattering of the Zeeman cooling beam, and then by the same effect reach the positive input of the 2D MOT with a velocity between 0 m/s and $-v_c$.

[0114] Contrary to the case of figure 11 (Nosske), in the first variant of the invention atoms with lower speeds comprised in the interval IS1 (atoms of zone 8) are decelerated such that to be trapped in the 2D-MOT.

[0115] The frequency detuning Δ_z m is thus determined so that a first set of atoms presenting speeds comprised in the first speed interval IS1 at the exit of the primary atom source and a second set of atoms presenting speeds comprised in the second speed interval IS2, with speeds of IS2 greater than the speeds of IS1, are decelerated because resonant with respectively a first and a second circular polarization component of the cooling beam. The second speed interval IS2 is contiguous to the first speed interval IS1.

[0116] For the case of a negative gradient as described here IS1 is resonant with σ^- and IS2 is resonant with σ^+ . For the case of a positive gradient IS2 is resonant with σ^- and IS1 is resonant with σ^+ .

[0117] The atom trajectories in the phase space corresponding to the optimal result for the set of parameters considered above (plus a saturation intensity for the Zeeman beam equal to 1.4) is determined by simulation and presented in figure 14. The optimal result is:

$$-\Delta_{7}/k = ~190 \text{ m/s}.$$

[0118] For strontium, where on the blue cooling transition k = 2 π / 461 nm = 1.36×10⁷ m⁻¹, it means a detuning Δ_{τ} m(opt)= - 414 MHz = -13.6 × Γ / 2 π .

[0119] To trap in the 2D MOT the two classes of atoms slowed down using the opposite polarization components of the cooling beam, it has been determined by simulation, for the first variant of the atom source according to the invention, that the detuning Δ_7 has to be in the interval:

$$-414 \text{ MHz} < \Delta_z m < -364 \text{ MHz}$$
 (4)

which in terms of linewidth of the cooling transition used for Sr is equivalent to -13.6 \times Γ / 2 π < Δ < -11.9 \times Γ / 2 π .

[0120] It can be seen on figure 14 compared to figure 11 (Nosske) that a much wider velocity interval of the atoms effused by the oven are trapped in the 2D-MOT. This result appears clearly in figure 15 showing the velocity distribution of atoms emitted by the oven (dark grey) at 585 °C and after the action of the trap is taken into account (light grey). The fraction of the Maxwell-Boltzman initial velocity distribution being captured by the 2D-MOT amounts to 26.9 % (peak 150).

[0121] This result is reduced to 9.3 % taking into account the radial losses (to compare with 4.1% of Nosske in figure

12). Indeed it can be seen on figure 14 that trajectory 140 is quite long and goes almost at the limit of zone 4. The long interval required to travel such a long distance determines a high radial extension of the atomic beam, which decreases substantially the flux of atoms effectively captured by the 2D-MOT.

[0122] The interval of formula (4) $IO_{Sr} = [-414 \text{ MHz}; -364 \text{ MHz}]$ for the detuning of the cooling beam has been determined by simulation with the following parameters:

- atom species = strontium: ∇B = - 40 G/cm; a_{max} = 9.3 10⁵ m/s²;

- saturation parameter of the cooling beam s=1.4 (ratio between the optical intensity of the cooling beam and the saturation intensity of the addressed atomic transition)

- 2D-MOT parameters of the example.

5

10

15

20

30

40

45

50

[0123] These parameters are subject to changes.

[0124] The values of the limits of the frequency internal for the detuning $\Delta_z m$ of the cooling beam depend at a first approximation mainly of the atom species (nominal magnetic field gradient required, value of a_{max} , properties of the cooling transition and most notably the wavevector k).

[0125] At a second level, once the atom species is fixed, the interval depends on parameter s. The interval is shifted toward high frequencies in absolute value when s increases.

[0126] The interval depends also on the value of the gradient. Still acceptable (but non optimized) results can be obtained by taking a gradient at +100 % /- 50% of the nominal value. For example for strontium it is 40 G/cm + 40 G/cm / 20 G/cm.

[0127] The 2D-MOT parameters (capture velocity, size, beam intensity and extension only slightly influence the values of the limits of the interval.

[0128] For strontium it has been established, by performing various simulations, that the frequency intervals for the detuning value, taking into account realistic values of s parameter and VB = -40 G/cm, are:

$$s=1:-400 \text{ MHz} < \Delta_z m < -350 \text{ MHz}$$

 $s=2:-430 \text{ MHz} < \Delta_7 \text{m} < -380 \text{ MHz}$

 $s=3:-460 \text{ MHz} < \Delta_z m < -405 \text{ MHz}$

 $s=4: -480 \text{ MHz} < \Delta_z m < -425 \text{ MHz}$

 $s=5:-500 \text{ MHz} < \Delta_z m < -445 \text{ MHz}$

 $s=10:-530 \text{ MHz} < \Delta_7 \text{m} < -480 \text{ MHz}$

55 [0129] A detuning in this the global interval I_{Sr} [-530 MHz; -350 MHz] allows a good trapping of atoms for reasonable values of s.

[0130] That is to say that the frequency detuning Δ_z m has to be comprised in an interval I depending on atom species.

[0131] The detuning value published by Nosske of $\Delta_z(N) = -210$ MHz for s=1.2 is out of this interval, and smaller in

absolute value.

5

10

15

20

25

30

35

50

55

[0132] Examples of atom species of interest have been listed in table I below with the key parameters of each species.

Table I

	⁸⁸ Sr	¹⁷⁴ Yb	⁴⁰ Ca	²⁴ Mg	¹¹⁴ Cd	²³ Na
MOT transition =cooling transition	¹ S ₀ - ¹ P ₁	3 ² S _{1/2} - 3 ² P _{3/2}				
λ _C (nm)	461	399	423	285.3	228	589
Γ (MHz)	2π 32	2π 28.9	2π 34.7	2π 80.95	2π 91 z	2π 9.79
I _{sat} (mW/cm ²)	42.5	63	59.9	455	1005	6.26
Typical ∇B Absolute value (G/cm)	40	60	60	100	80	40
a _{max} (m/s ²)	10 ⁵	5.2 10 ⁵	25.5 10 ⁵	148 10 ⁵	46.4 10 ⁵	9.0 10 ⁵

[0133] For each atom species of interest of table I, associated with possible s coefficient and gradient values, the inventor has established by simulation an associated suitable interval I for the cooling beam detuning Δ_z .

[0134] For sodium and for the saturation parameter s=6.5 as adopted in Lamporesi the interval has been calculated by simulation and gives an interval [-362 MHz; - 333 MHz]. This interval is out of the detuning value of -304 MHz published by Lamporesi, smaller in absolute value.

[0135] A saturation parameter lower than s=5 is not suitable, because the high atom velocities that should be decelerated at the beginning of region 2 do not scatter enough photons to remain in resonance along the magnetic field slope, and then they are not finally trapped by the 2D MOT.

[0136] With VB = -40 G/cm:

$$s=5:-350 \text{ MHz} < \Delta zm < -325 \text{MHz}$$

$$s=6:-355 \text{ MHz} < \Delta zm < -330 \text{ MHz}$$

$$s=7:-360 \text{ MHz} < \Delta zm < -335 \text{ MHz}$$

$$s=10: -375 \text{ MHz} < \Delta zm < -350 \text{ MHz}$$

[0137] A detuning in this the global interval I_{Na}: [-360 MHz; -325 MHz] allows a good trapping of atoms for reasonable values of s.

[0138] Similarly for Ytterbium a saturation parameter lower than s=5 is not suitable, because the high atom velocities that should be decelerated at the beginning of region 2 do not scatter enough photons to remain in resonance along the magnetic field slope, and then they are not finally trapped by the 2D MOT.

[0139] With VB = -60 G/cm:

$$s=5:-560MHz < \Delta_7 m < -520MHz$$

$$s=6:-575 \text{ MHz} < \Delta_z m < -535 \text{ MHz}$$

$$s=7:-590 \text{ MHz} < \Delta_z m < -550 \text{MHz}$$

$$s=10:-620 \text{ MHz} < \Delta_z m < -565 \text{ MHz}$$

[0140] A detuning in this the global interval I_{Yb} : [-620 MHz; -520 MHz] allows a good trapping of atoms for reasonable values of s

[0141] For calcium a saturation parameter lower than s=0.7 is not suitable, because the high atom velocities that should be decelerated at the beginning of region 2 do not scatter enough photons to remain in resonance along the magnetic field slope, and then they are not finally trapped by the 2D MOT.

[0142] With VB = -40 G/cm:

10

15

30

35

40

50

55

 $s=1:-610 \text{ MHz} < \Delta_7 \text{m} < -525 \text{ MHz}$

 $s=2:-660 \text{ MHz} < \Delta_z m < -575 \text{ MHz}$

 $s=3:-695 \text{ MHz} < \Delta_z m < -610 \text{ MHz}$

 $s=5:-750 \text{ MHz} < \Delta_7 \text{m} < -660 \text{ MHz}$

20 [0143] A detuning in this the global interval I_{Ca}: [-695 MHz; -525 MHz] allows a good trapping of atoms for reasonable values of s.

[0144] For magnesium a saturation parameter lower than s=0.1 is not suitable, because the high atom velocities that should be decelerated at the beginning of region 2 do not scatter enough photons to remain in resonance along the magnetic field slope, and then they are not finally trapped by the 2D MOT.

[0145] With VB = -100 G/cm :

 $s=0.1:-970 \text{ MHz} < \Delta_z m < -875 \text{ MHz}$

 $s=0.2:-1075 \text{ MHz} < \Delta_z m < -945 \text{ MHz}$

 $s=0.3: -1155 \text{ MHz} < \Delta_7 \text{m} < -1000 \text{ MHz}$

 $s=0.5:-1271 \text{ MHz} < \Delta_7 \text{m} < -1070 \text{ MHz}$

[0146] A detuning in this the global interval I_{Mg}: [-1271 MHz; -875 MHz] allows a good trapping of atoms for reasonable values of s.

[0147] For cadmium a saturation parameter lower than s=0.1 is not suitable, because the high atom velocities that should be decelerated at the beginning of region 2 do not scatter enough photons to remain in resonance along the magnetic field slope, and then they are not finally trapped by the 2D MOT. Given the very high saturation intensity lsat=1005 mW/cm2 it is not interesting to evaluate the case of s>0.3.

45 **[0148]** With VB = -80 G/cm:

 $s=0.1:-810 \text{ MHz} < \Delta_7 \text{m} < -720 \text{ MHz}$

 $s=0.2:-910 \text{ MHz} < \Delta_7 \text{m} < -790 \text{ MHz}$

 $s=0.3: -970 \text{ MHz} < \Delta_7 \text{m} < -835 \text{ MHz}$

[0149] A detuning in this the global interval I_{Cd}: [-720 MHz; -970 MHz] allows a good trapping of atoms for reasonable values of s.

[0150] More generally the detuning according to the first variant of the invention, and considering the atom species of

interest, is comprised in a global interval of [-1271 MHz; -325 MHz]. Taking into account variations of the gradient around the nominal values (mainly above the nominal value which more interesting in terms of captured atom flux) the global interval becomes:

 $I_G \cong [-1500 \text{ MHz}; -325 \text{ MHz}].$

[0151] For other atom species of interest having physical parameters of the same order of magnitude as the atom species given above, the value of the interval is also I_G .

[0152] In order to minimize the atomic losses caused by the radial expansion of the thermal atomic beam, it is necessary to drastically shorten the long trajectories previously being inverted in region 4 (see trajectory 140 on figure 14). This is obtained by making asymmetric the maximum value and the minimum value of the magnetic field. An example of a cold atom source 11 according to the second variant of the invention is shown on figure 16. Figure 16 A shows the setup configuration.

[0153] The magnetic device MD of cold atom source according to the second variant of the invention is configured to generate a magnetic field By varying along z between two extrema, a positive maximum and a negative minimum, the absolute value of the extremum located on a side opposite to the atom primary source being strictly greater than an absolute value of the other extremum. With such asymmetric values of the magnetic field the position on the z axis of the extremum located on the side opposite to the primary atom source has to be determined in order to keep a null value on the centre O.

[0154] In the example of figure 16 for strontium with a negative gradient $\nabla B \sim 40$ G/cm, $B_{max} \sim 160$ G at -z0 = -5 cm and Bmin ~ -230 G at z0 = 6.23 cm (see figure 16 B). It is the minimum which is located on the side opposite to the oven and the condition is:

|Bmin|>Bmax.

5

10

15

20

30

35

50

55

[0155] For the case of a positive gradient VB \sim + 40 G/cm, it is the positive maximum which is located on the side opposite to the oven. In this case the condition is: Bmax > |Bmin|.

[0156] In an embodiment of the second variant of the invention shown on figure 16 the magnetic device MD comprises four sets of stacked permanent magnets. To keep the null value at O the four sets are arranged at the corners of a rectangle R' in the xz plane centred in a point O' located on the z axis but offset from O. The two sets (S3, S4) are arranged on the primary source side, and the two sets (S1, S2) are arranged on the other side. The two sets (S3, S4) and the two sets (S1, S2) have respective magnetic dipoles oppositely oriented along the y axis. And the absolute value M2 of the magnetic dipoles of (S3, S4) is smaller than the absolute value M1 of the two sets (S1, S2) (see figure 16 C).

[0157] In the example of figure 16 the sets (S1, S2) are located at z1=+6.23 mm and the sets (S3, S4) at -z0=-5 cm. [0158] The cold atom source according to the second variant of the invention also comprises a cooling beam CBm propagating in a direction opposite to that of the atoms. The cooling beam presents a frequency detuning with respect to a frequency of a cooling transition having a negative value Δ_z m depending on the atom species (see further).

[0159] Figure 17 shows a phase-space plot with the atomic trajectories for the atoms effused by the oven at z=-15 modified by the combined effect of the magnetic field generating the linear quadrupole for the 2D-MOT along the y axis at z=0, and the Zeeman slowing beam CBm opposite to the atomic beam and with a detuning Δz with respect to the cooling transition, for a cold atom source according to the second variant of the invention. For the simulation the parameters are identical to those of figure 13 except the magnetic field configuration.

[0160] Curve 15 shows in the phase space the atoms being in resonance with the σ^+ polarization component of the cooling beam (detuning Δ_z), and curve 14 shows in the phase space the atoms being in resonance with the σ^- polarization component of the cooling beam. Zone 12 shows the atoms emitted by the oven with a speed (at the exist of the oven) comprised in a first interval IS1' that makes them enter in resonance with the σ^- Zeeman beam component in region 1, and there be decelerated until z=-z0= -5cm. Zone 13 shows the atoms emitted by the oven with a speed comprised in a second interval IS2' that makes them enter in resonance with σ^+ Zeeman beam component in region 2, to be there and in region 3 decelerated until z= z0 =6.23 cm.

[0161] Here also the frequency detuning Δ_z m is thus determined so that a first set of atoms presenting speeds comprised in the first speed interval IS1' at the exit of the primary atom source and a second set of atoms presenting speeds comprised in the second speed interval IS2', with speeds of IS2' greater than speeds of IS1', are decelerated because resonant with respectively a first and a second circular polarization component of the cooling beam. For the case of a negative gradient as described here IS1' is resonant with σ^- and IS2' is resonant with σ^+ . The two intervals IS1' are IS2' are also contiguous.

[0162] Here the cooling beam at a detuning Δz is resonant with with atoms moving along the z axis at velocity $-\Delta z/k$ wherever the B field is null, condition verified at z=0 (i.e. the 2D MOT position), and well approximated far from the

magnet configuration (i.e. at the oven and where the cooling beam enters the setup).

10

25

30

35

40

45

50

55

[0163] Elsewhere the cooling beam is resonant with a velocity that depends on the local magnetic field, which shifts the atomic levels.

[0164] More precisely, it is resonant with velocities from $-\Delta/k + \mu_B B_{max}/(\hbar k)$ to $-\Delta/k$ in region 1 via its σ^- polarization component, and from $-\Delta/k$ to $-\Delta/k + \mu_B B_{max}/(\hbar k)$ in region 2 via its σ^+ polarization component.

[0165] The two groups of atoms cooled by the opposite polarizations are bouched in velocity at the end of the respective slope:

- the atoms cooled in region 1 are at z=-5 cm (position of the magnet stacks close to the oven) with v= - Δ/k + μ_B B_{max}/(\hbar k),
- the atoms cooled in region 2 from z=0 are decelerated in region 3 until at z=6.23 cm (position of the magnet stacks far from the oven) have v= $-\Delta/k + \mu_B B_{min}/(\hbar k)$.

[0166] The main difference with the symmetric configuration is related to the lower output velocity of the atoms decelerated in regions 2 and 3, which permits them to reach the 2D MOT capture region without a long trajectory in region 4. As a consequence, the efficiency of the configuration is higher, given the lower impact of the radial beam expansion in terms of atom losses.

[0167] The atom trajectories in the phase space corresponding to the optimal result for the set of parameters considered above (plus a saturation intensity for the Zeeman beam equal to s= 1.4) is determined by simulation and presented in figure 18. The optimal result is:

$$-\Delta_{7}/k = ~205 \text{ m/s}.$$

[0168] For strontium, where on the blue cooling transition k = 2 π / 461 nm = 1.36×10⁷ m⁻¹, it means a detuning Δ_z m(opt)= - 445 MHz = -14.5 × Γ / 2 π .

[0169] To trap in the 2D MOT the two classes of atoms slowed down using the opposite polarization components of the cooling beam, it has been determined by simulation, for the first variant of the atom source according to the invention, that the detuning Δ_z has to be in the interval:

$$10_{Sr}^* = -445 \text{ MHz} < \Delta_z m < -365 \text{ MHz}$$

which in terms of linewidth of the cooling transition used for Sr is equivalent to :

$$-14.6 \times \Gamma/2 \pi < \Delta < -12 \times \Gamma/2 \pi$$
.

[0170] The values of the limits of interval 10_{Sr}^* are slightly different from the one obtained for the first variant of the invention (10_{Sr} = [-414 MHz; -364 MHz]).

[0171] It can be seen on figure 18 that trajectories previously located in region 4 (see figure 14 trajectory 140) are reduced (see trajectory 180). The asymmetric magnetic field has the effect of shortening the atomic trajectories ending in the 2D-MOT after being decelerated in regions 2 and 3.

[0172] Figure 19 shows the velocity distribution of atoms emitted by the oven (dark grey) at 585 °C and after the action of the trap is taken into account (light grey). The fraction of the Maxwell-Boltzman initial velocity distribution being captured by the 2D-MOT amounts to 26.9 % (see peak 190). Given the shorter interval taken by these atoms to go from the oven to the final trapping region, a smaller fraction is lost because of the radial expansion of the atomic beam: when losses are taken into account, the fraction of atoms captured by the 2D MOT drops from 26.9% to 14.8%, which represent -60% (=14.8% / 9.3%) more with respect to the setup with the symmetric field configuration.

[0173] The inventor has also established by simulation that good results are obtained with: |Bmin| / Bmax = K (negative gradient) or Bmax / |Bmin| = K (for positive gradient) with K comprised between 1.3 and 3.

[0174] That is to say that the absolute value of the magnetic field on the side opposite to the primary atom source has to be equal to K times the absolute value of the magnetic field on the side of the primary atom source.

[0175] The lower limit is set to get an effect on the atomic flux.

[0176] The upper limit is set by the encumbrance of the permanent magnet stack and by the disturbance determined by a large magnetic field on the rest of the apparatus, and is set to a ratio of 3. Note that a ratio of 5 gives an atomic source according to the invention, but having such a large and not necessary magnetic field is not very suitable in a cold atom experiment.

[0177] For each species, in this second variant of the invention the values of the limits of the interval I* is slightly different in frequency with respect to the interval I determined for the first variant of the invention. Each interval has to be determined by simulation.

[0178] More generally the detuning according to the second variant of the invention, and considering the atom species of interest, is comprised in a global interval of [-1330 MHz; -325 MHz]. Taking into account variations of the gradient around the nominal values (mainly above the nominal value which more interesting in terms of captured atom flux) the global interval becomes:

$I_{G}^{*} \cong [-1500 \text{ MHz}; -325 \text{ MHz}].$

[0179] For other atom species of interest having physical parameters of the same order of magnitude than the atom species given above, the value of the interval is also I_{G^*} .

[0180] Thus the evaluation of the limits of global intervals I_G and I_G^* are similar.

10

15

30

35

40

50

[0181] To further increase the velocity interval captured in the 2D-MOT according to an embodiment of the invention the cooling beam CBm presents an additional frequency detuning Δ_z m' determined from the frequency detuning Δ_z m. This embodiment is compatible with the first and the second variant of the invention.

[0182] Figure 20 shows a phase-space plot with the atomic trajectories for the atoms according to this embodiment, in combination with the second variant of the invention. The trajectories of the atoms effused by the oven at z=-15 are modified by the combined effect of the magnetic field generating the linear quadrupole for the 2D-MOT along the y axis at z=0, and of the Zeeman slowing beam CBm opposite to the atomic beam, the cooling beam CBm presenting an initial detuning Δ_z with respect to the cooling transition, and an additional detuning Δ_z correctly chosen.

[0183] Curve 16 shows in the phase space the atoms being in resonance with the σ^+ polarization component of the cooling beam of detuning Δ_z , and curve 17 shows in the phase space the atoms being in resonance with the σ^- polarization component of the cooling beam of detuning Δ_z . A third set of atoms with speed comprised in a third speed interval IS3' are captured by the 2D-MOT.

[0184] Similar results can be obtained by combining the additional detuning Δ_z with the initial detuning Δ_z for the first variant of the invention (third speed interval IS3). IS3' is contiguous to IS2'.

[0185] Figure 21 shows the calculated trajectories in the phase space corresponding to the optimal result for the set of parameters considered above (saturation intensity for the Zeeman beam equal to s= 1.4, for the second variant of the invention.

[0186] The first detuning is $\Delta_z m$ = -445 MHz (equal to -14.5 $\Gamma/(2\pi)$ for strontium) and the additional second detuning is $\Delta_z m$ = -884 MHz (equal to -29.0 $\Gamma/(2\pi)$ for strontium). Atoms with a velocity between 330 m/s and 550 m/s are decelerated in region 1 (i.e. between z=-15 cm and z=-5 cm) by interacting with the σ - polarization component of the second cooling beam frequency (frequency with detuning Δ_z '), and join then the atoms with speed in the interval IS2' being decelerated in regions 2 and 3 by interacting with the σ + polarization component of the first cooling beam frequency (frequency with detuning Δ_z).

[0187] Figure 22 shows the corresponding velocity distribution of atoms emitted by the oven (dark grey) at 585 °C and after the combined action of the Zeeman slower and 2D-MOT is taken into account (light grey). The fraction of the initial Maxwell-Boltzmann velocity distribution for an atomic temperature T=585oC being captured by the 2D MOT amounts to 52.8%, reduced to 26.4% because of the radial losses. The atom flux captured by the 2D-MOT is increased compared to the one without the additional detuning.

[0188] It has been established that starting from an initial detuning value Δ_z m the additional detuning is calculated by the formula :

$$\Delta_z m0' = \Delta_z m - 2 \,\mu_B \,B_{PSS} / \,\hbar - 2 \,\Gamma/(2\pi) \tag{5}$$

with μ_B the Bohr magneton, \hbar the Planck constant and $\Gamma/(2\pi)$ the natural linewidth of the atom species, and B_{PSS} is the absolute value of the magnetic field extremum located on the primary atom source side.

[0189] With a negative gradient B_{PSS} = Bmax, and with a positive gradient B_{PSS} = |Bmin|.

[0190] But a tolerance exists and the additional detuning Δ_7 m' can be chosen in the interval defined by:

$\Delta_z m' = \Delta_z m 0' + 2 \Gamma/(2\pi) = \Delta_z m - 2 \mu_B B_{PSS} / \hbar - 2 \Gamma/(2\pi) + 2 \Gamma/(2\pi)$ (6)

Claims

5

10

15

20

25

30

40

45

50

55

- 1. Cold atom source (10) comprising:
 - a primary atom source (PAS) configured to generated an atomic beam (AtB) propagating along a z direction of a coordinate system xyz,
 - a two-dimensional magneto-optical trap, called 2D-MOT, comprising :
 - ❖ a first pair (LB1, LB1') and a second pair (LB2, LB2') of two counter-propagating beams, the two pairs being perpendicular to each other and located in a plane yz, the intersection of which defining a trap zone (ZTr) having a centre O,
 - ❖ a magnetic device (MD) configured to generate a magnetic field having :
 - a null value at centre O and on the x axis at least inside the trap zone,
 - a component along y By having a gradient along the z axis being almost constant in the trap zone, an absolute value of said constant depending on the atom species,
 - the component along y By varying along the z axis between two extrema, a positive maximum and a negative minimum, said positive maximum and said negative minimum having identical absolute values,
 - a cooling beam (CBm) propagating in a direction opposite to that of the atoms, the cooling beam presenting a frequency detuning with respect to a frequency of a cooling transition having a negative value Δ_z m depending on the atom species, said frequency detuning being determined so that a first set of atoms presenting speeds comprised in a first speed interval (IS1) at an exit of the atom primary source and a second set of atoms presenting speeds comprised in a second speed interval (IS2) greater than the speeds of the first interval, are decelerated by resonance with respectively a first and a second circular polarization component of the cooling beam, the second speed interval (IS2) being contiguous to the first speed interval (IS1).
- 2. The cold atom source as claimed in the preceding claim wherein the magnetic device comprises two sets (S1t, S2t) of stacked permanent magnets, respectively arranged along the y axis symmetrically on either side of the z axis and having respective magnetic dipoles oppositely oriented along the z axis.
 - 3. The cold atom source as claimed in claim 1 wherein the magnetic device comprises four sets of stacked permanent magnets, arranged at the corners of a rectangle (R) in the xz plane centred in O, the two sets (S3, S4) arranged on the primary source side and the two sets arranged on the other side (S1, S2) having respective magnetic dipoles oppositely oriented along the y axis.
 - **4.** Cold atom source (11) comprising:
 - a primary atom source (PAS) configured to generated an atomic beam (AtB) propagating along a z direction of a coordinate system xyz,
 - a two-dimensional magneto-optical trap, called 2D-MOT, comprising :
 - ❖ a first pair (LB1, LB1') and a second pair (LB2, LB2') of two counter-propagating beams, the two pairs being perpendicular to each other and located in a plane yz, the intersection of which defining a trap zone (ZTr) having a centre O,
 - ❖ a magnetic device (MD) configured to generate a magnetic field having :
 - a null value at centre O and on the x axis at least inside the trap zone,
 - a component along y By having a gradient along the z axis being constant in the trap zone, an absolute value of said constant depending on the atom species,
 - the component along y By varying along the z axis between two extrema, a positive maximum and a negative minimum, an absolute value of the extremum located on a side opposite to the primary atom

source being strictly greater than an absolute value of the other extremum,

5

10

15

20

25

40

45

50

55

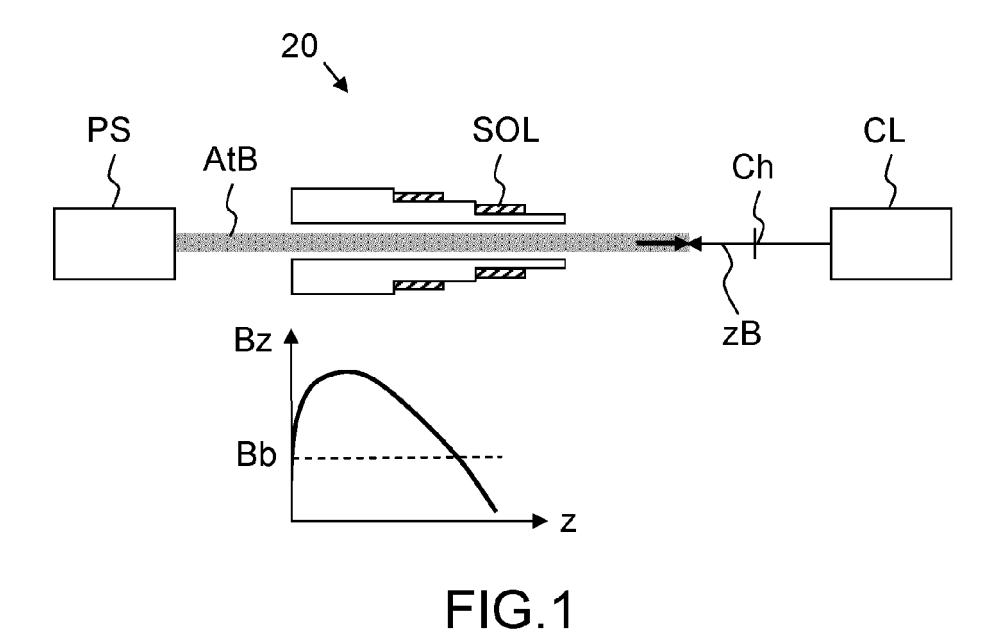
- a cooling beam (CBm) propagating in a direction opposite to that of the atoms, the cooling beam presenting a frequency detuning Δ_z m with respect to a frequency of a cooling transition having a negative value depending on the atom species.
- 5. The cold atom source as claimed in the preceding claim wherein the absolute value of the extremum located on the side opposite to the primary atom source is strictly greater than the absolute value of the other extremum, of a factor (K) being comprised between 1.3 and 3.
- 6. The cold atom source as claimed in one of the claims 4 or 5 whereas the magnetic device comprises four sets of stacked permanent magnets arranged at the corners of a rectangle (R') in the xz plane centred in a point O' located on the z axis but offset from O, the two sets (S3, S4) arranged on the primary source side and the two sets arranged on the other side (S1, S2) having respective magnetic dipoles oppositely oriented along the y axis, and an absolute value (M2) of the magnetic dipoles of the two sets arranged on the primary source side (S3, S4) being smaller than an absolute value (M1) of the two sets (S1, S2) arranged on the other side.
- 7. The cold atom source as claimed in one of the preceding claims wherein the cooling beam (CBm) presents an additional frequency detuning Δ_z m' determined from the frequency detuning Δ_z m by the formula :

$$\Delta_z m' = \Delta_z m - 2 \mu_B B_{PSS} / \hbar - 2 \Gamma/(2\pi) + /- 2 \Gamma/(2\pi)$$

- with μ_B the Bohr magneton, \hbar the Planck constant and $\Gamma/(2\pi)$ the natural linewidth of the atom species, and B_{PSS} is the absolute value of the magnetic field extremum located on the primary atom source side.
- **8.** The cold atom source as claimed in one of the preceding claims wherein the atom species is chosen among: Strontium; Ytterbium; Calcium; Magnesium; Cadmium; Sodium.
- 30 **9.** The cold atom source as claimed in one of the preceding claims wherein the frequency detuning Δ_{τ} m is such that :

$-1500 \text{ MHz} \le \Delta_z \text{m} \le -325 \text{ MHz}$

- 10. The cold atom source as claimed in one of the preceding claims wherein the primary atom source is an oven.
 - **11.** The cold atom source as claimed in one of the claims 1 to 9 wherein the primary atom source is a solid atomic source whose desorption is controlled by a laser source.



LŖ1 LB2 **→** Z LB2'

LB1'

AtB

FIG.2A

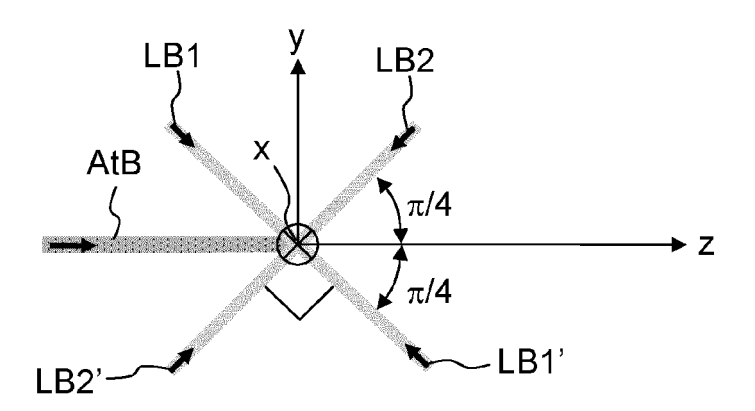


FIG.2B

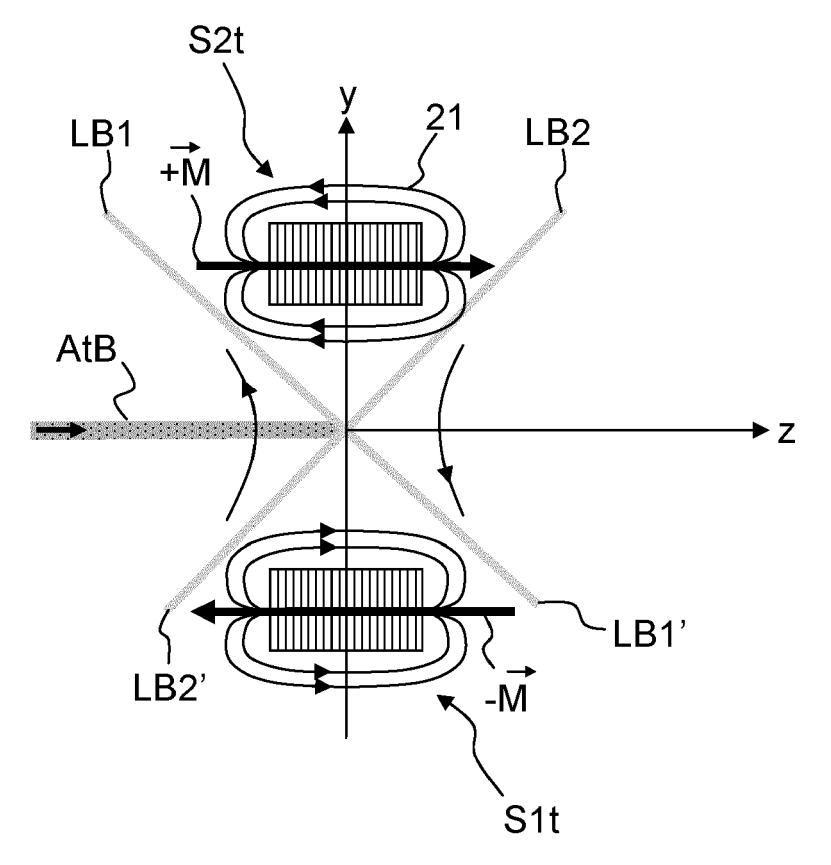


FIG.2C

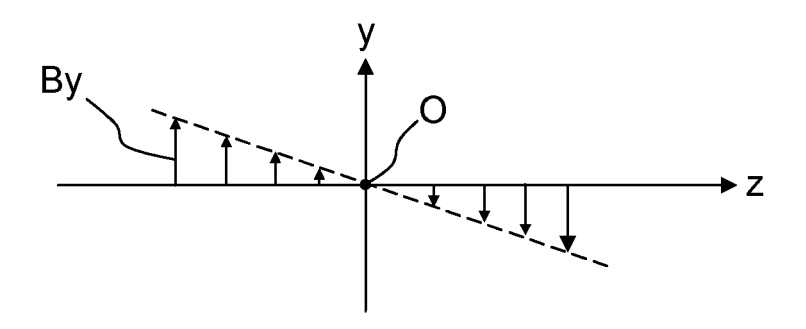
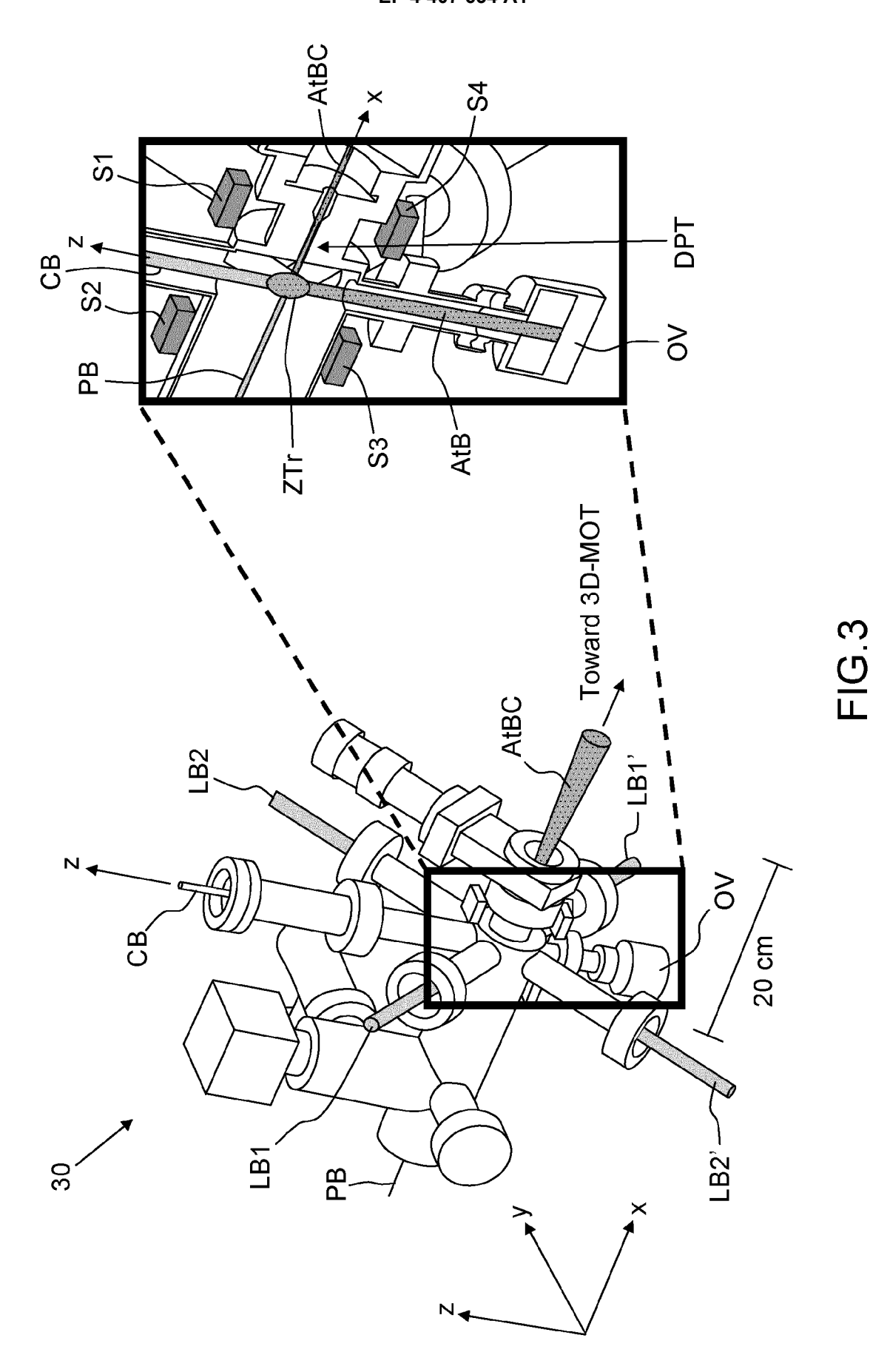


FIG.2D



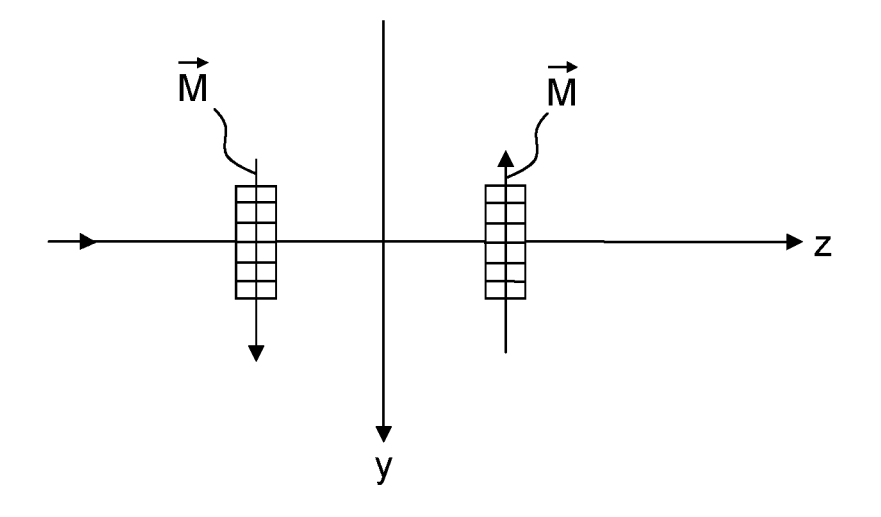


FIG.4

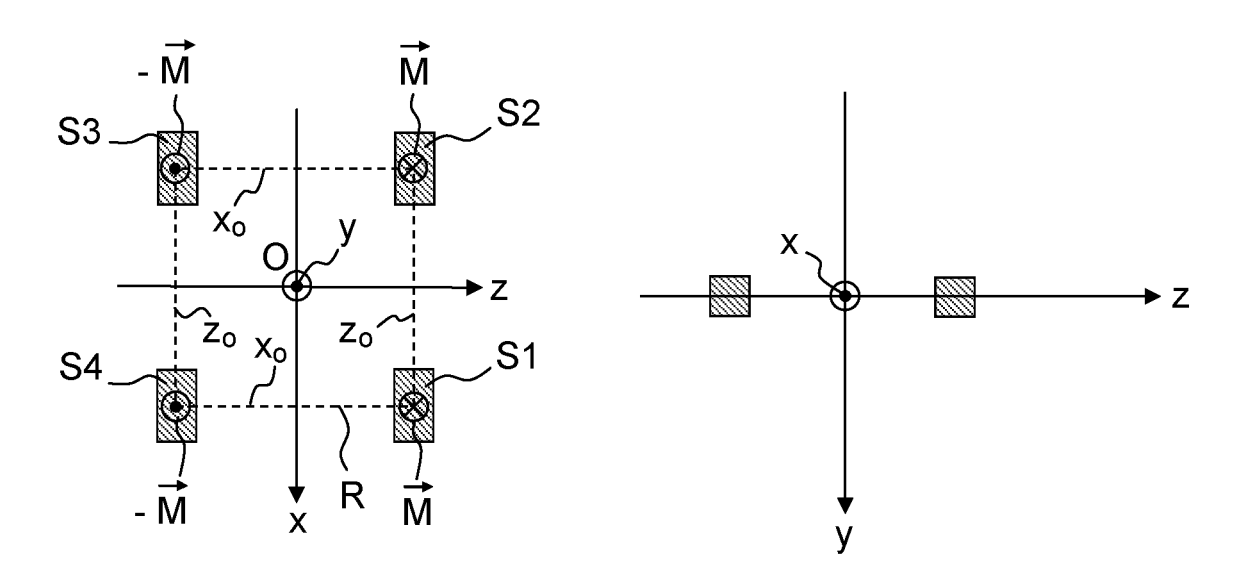


FIG.5

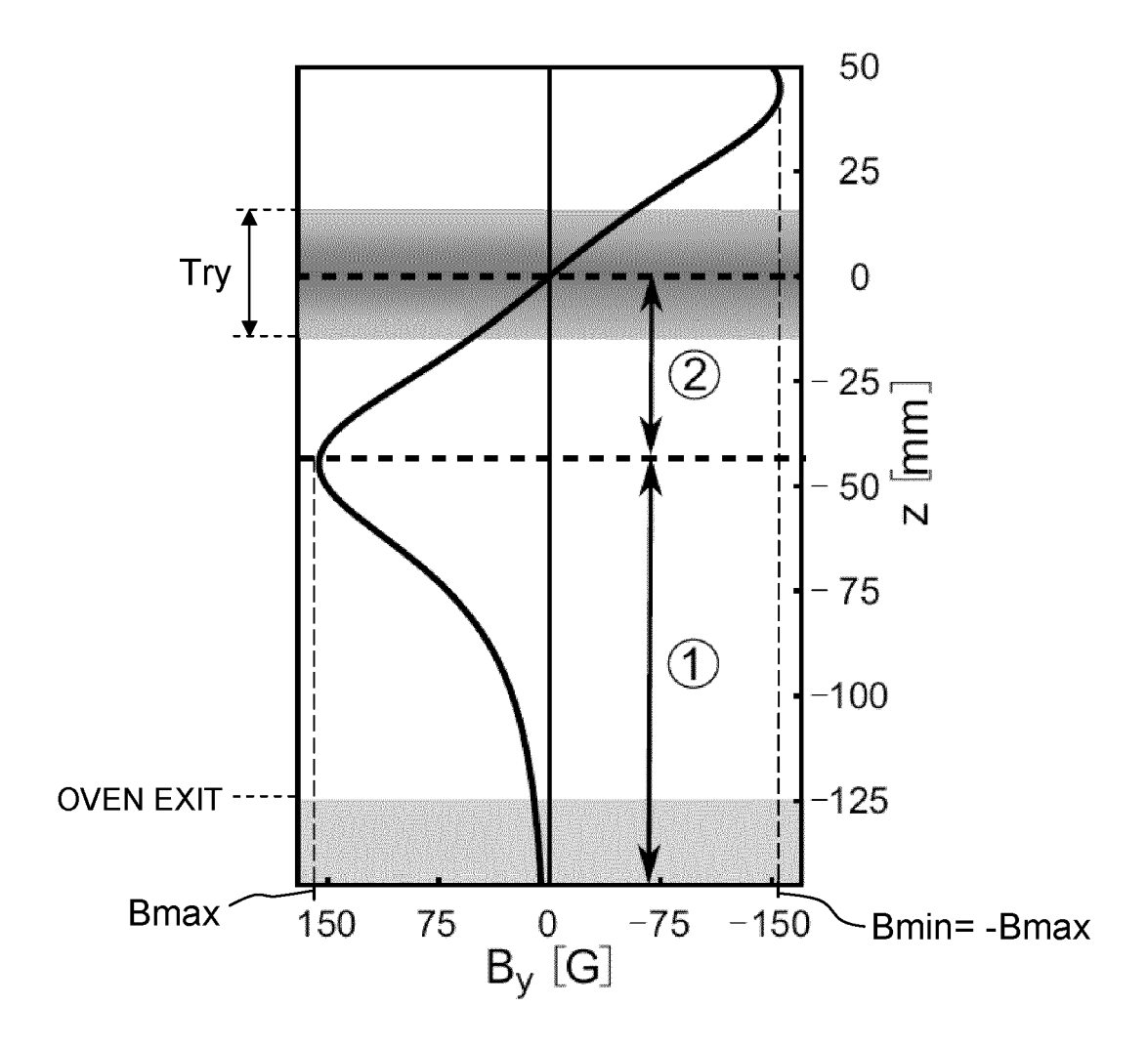


FIG.6

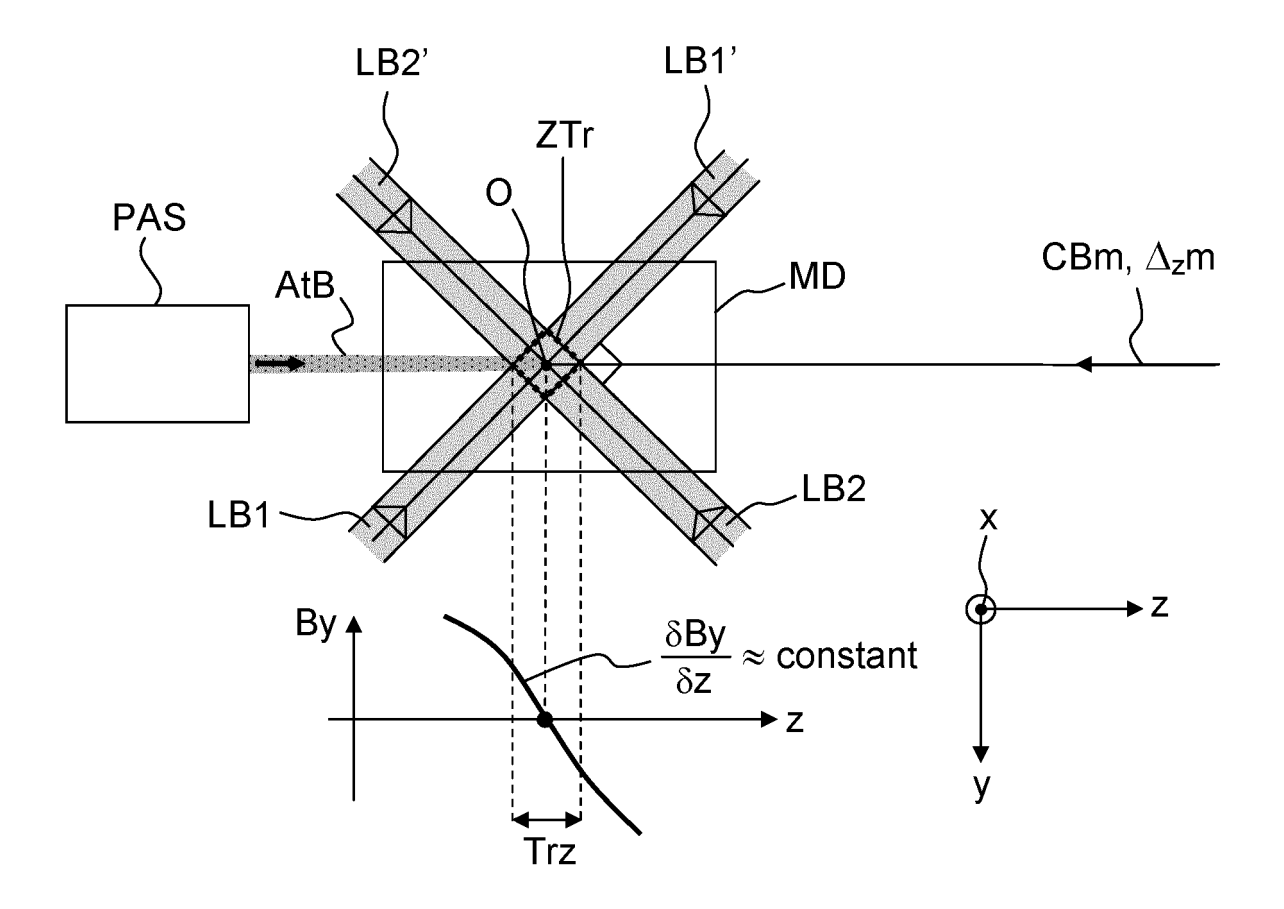
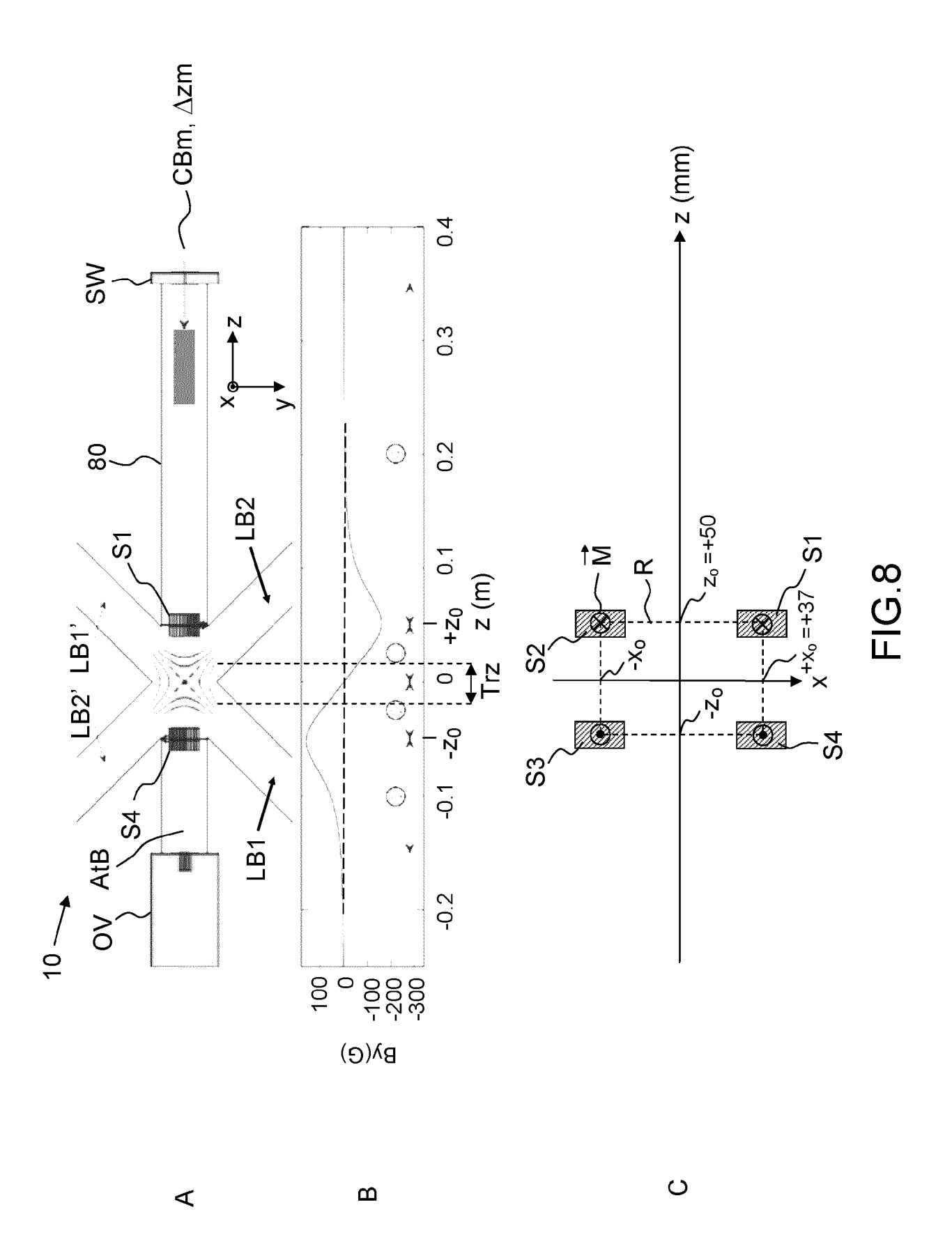
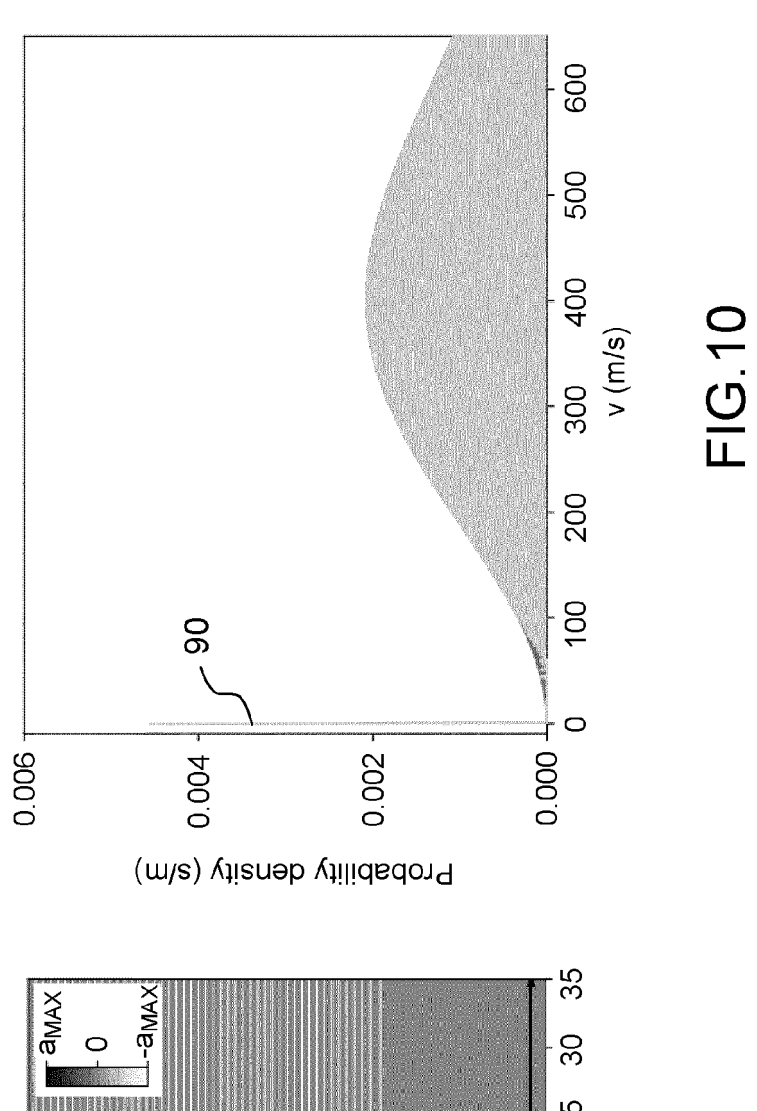
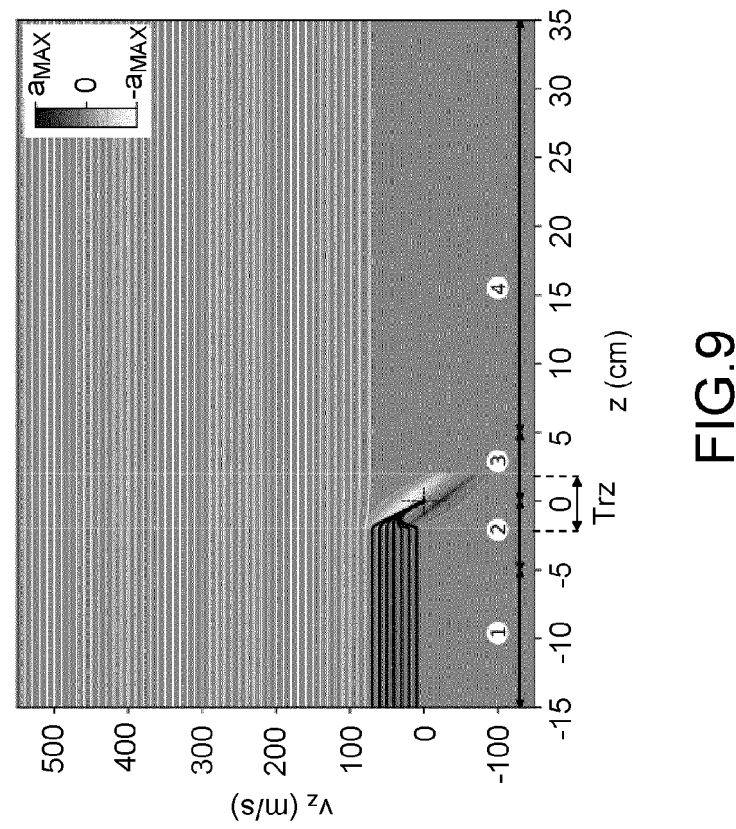
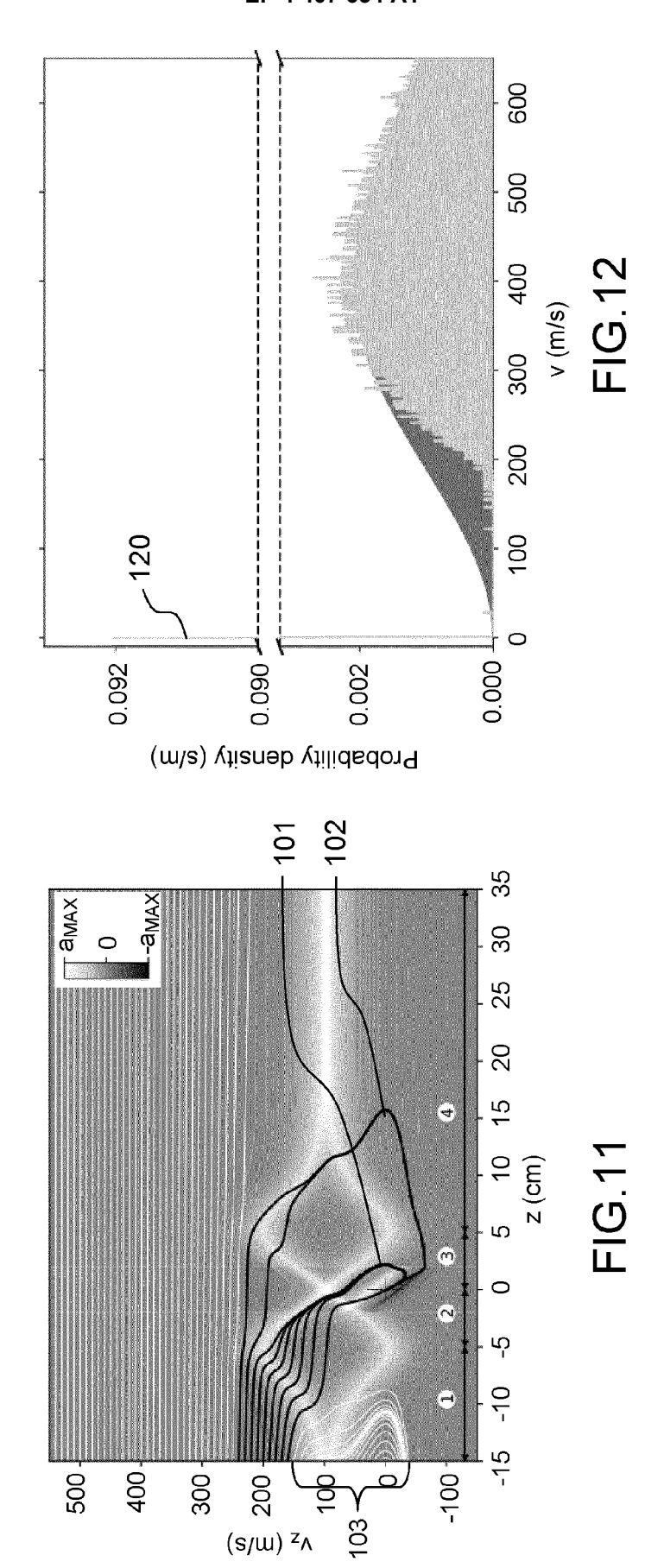


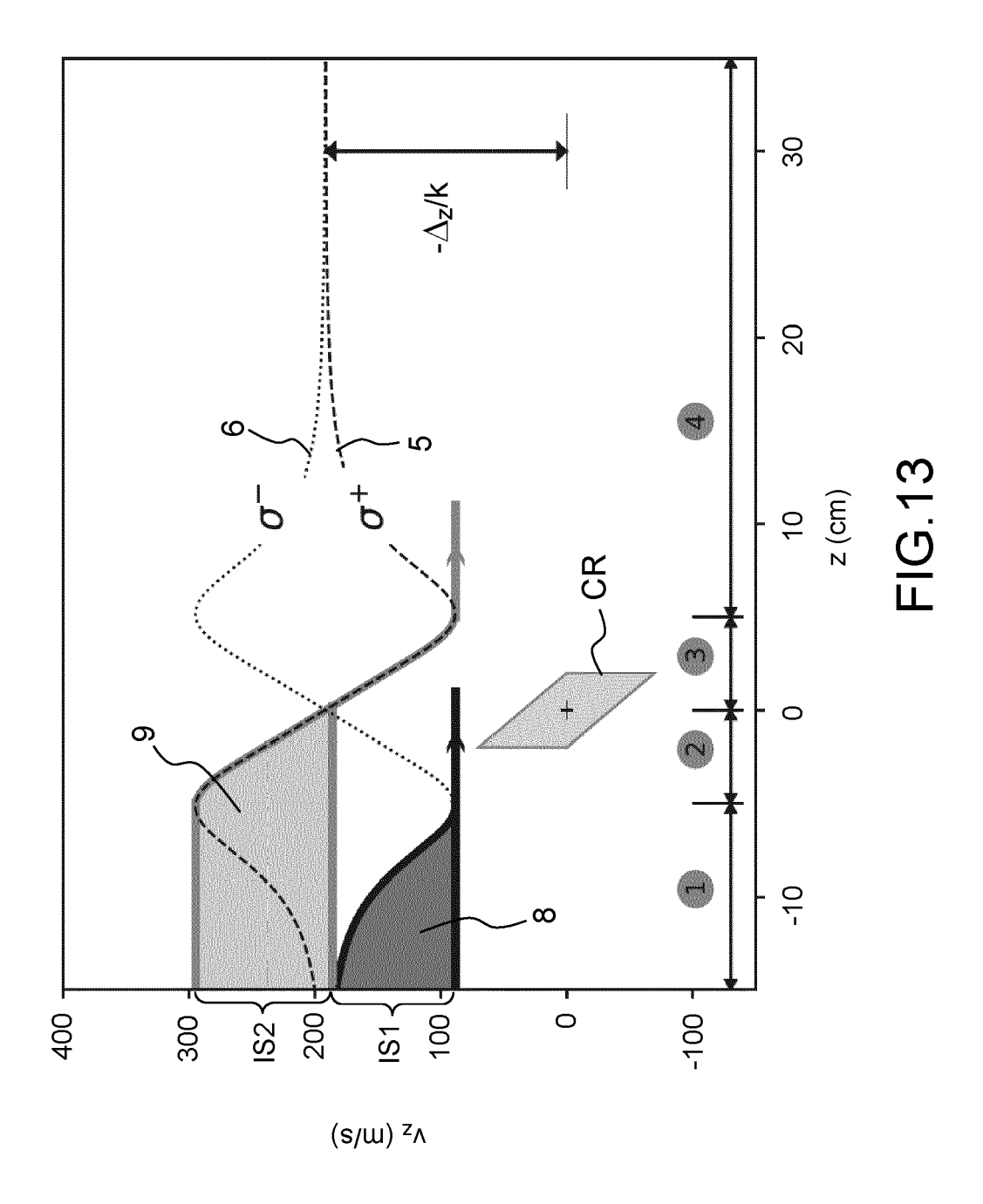
FIG.7

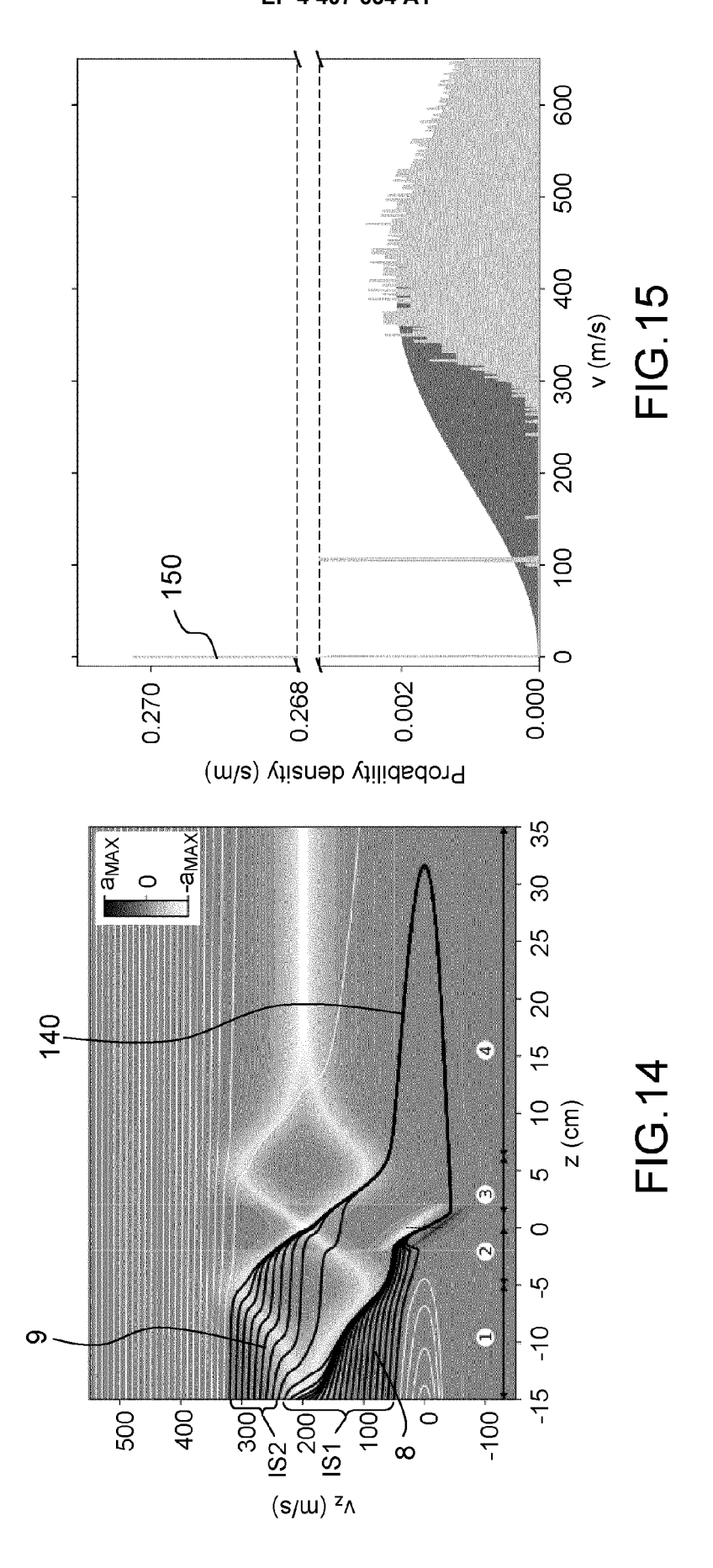


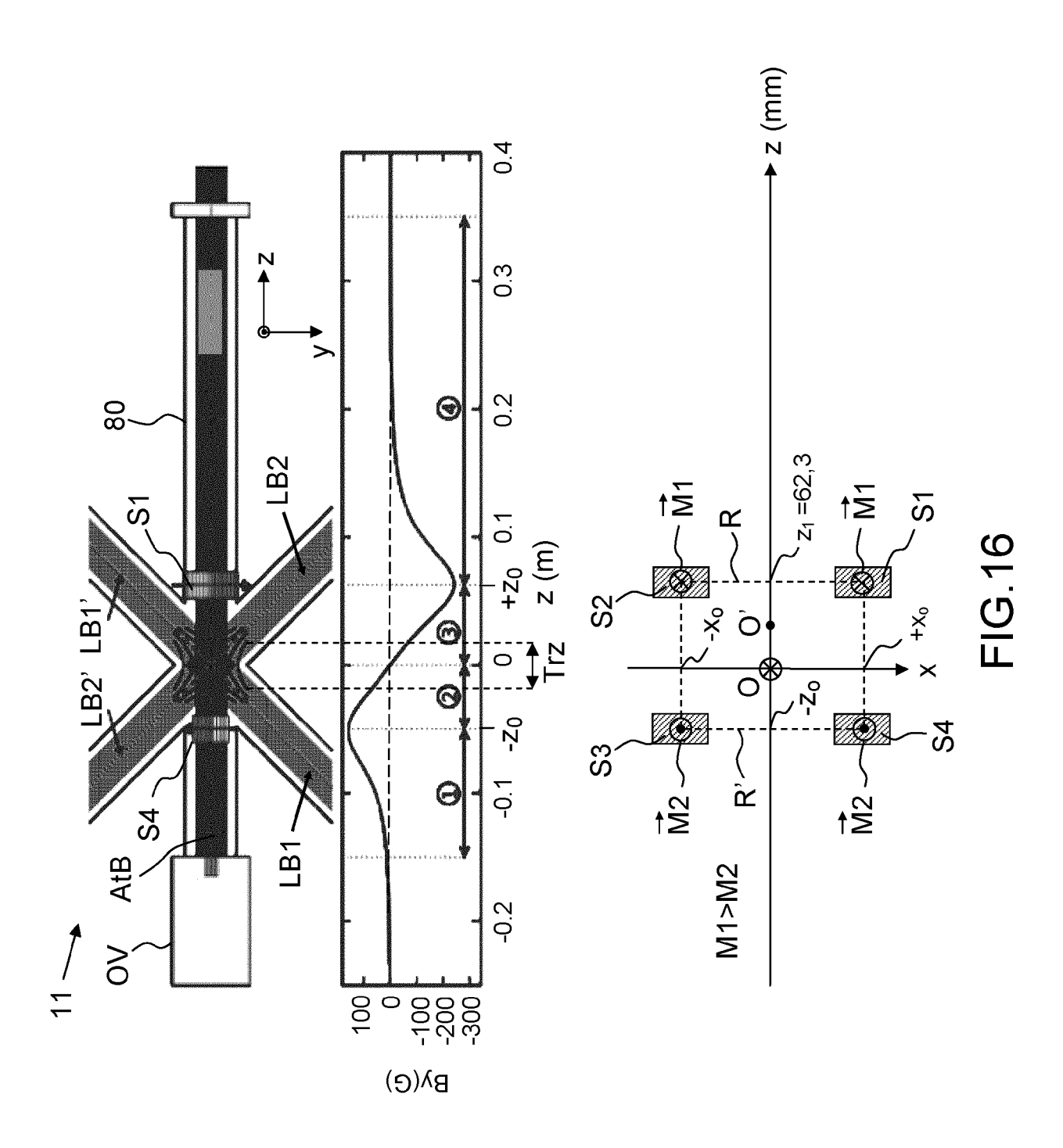




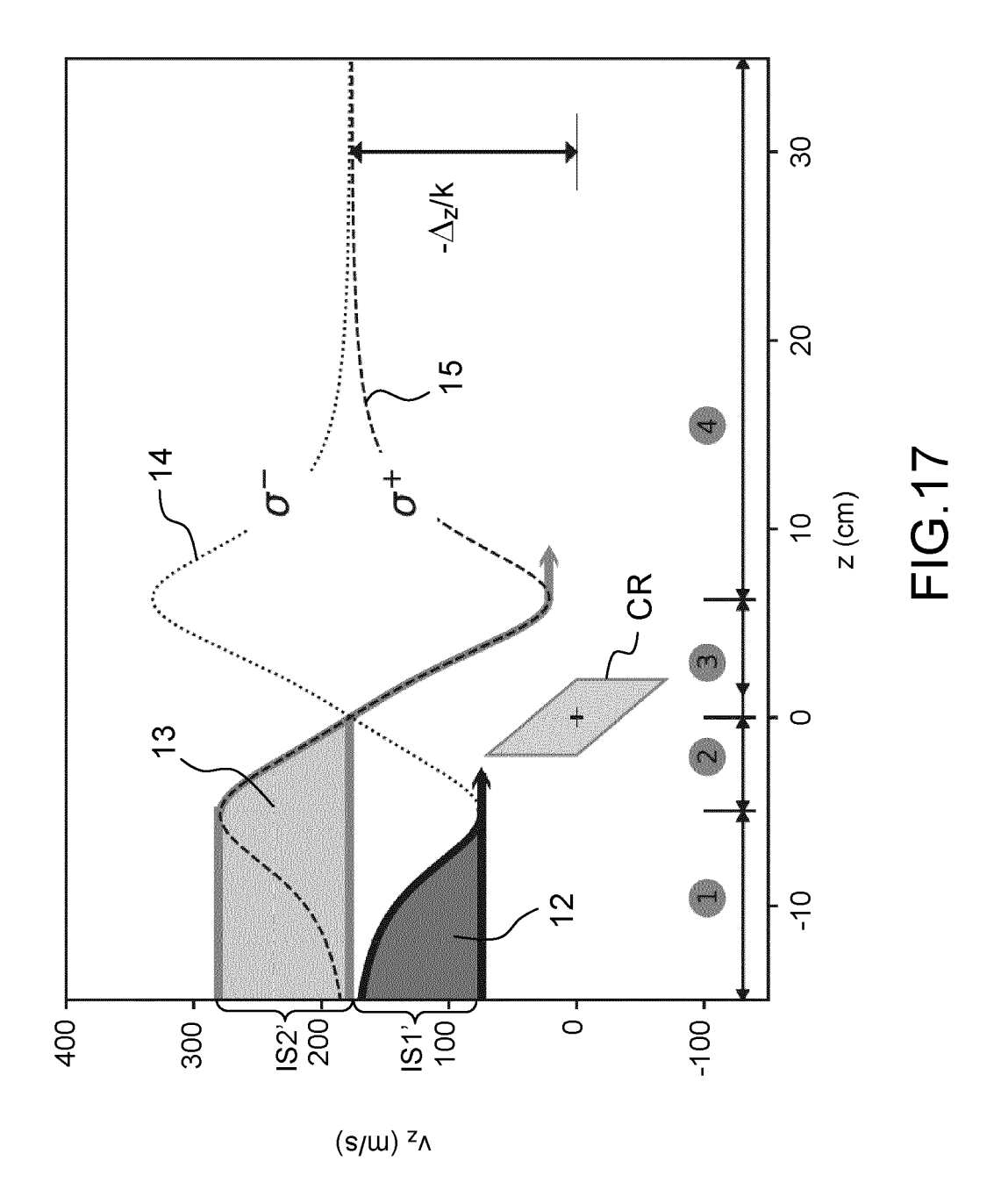


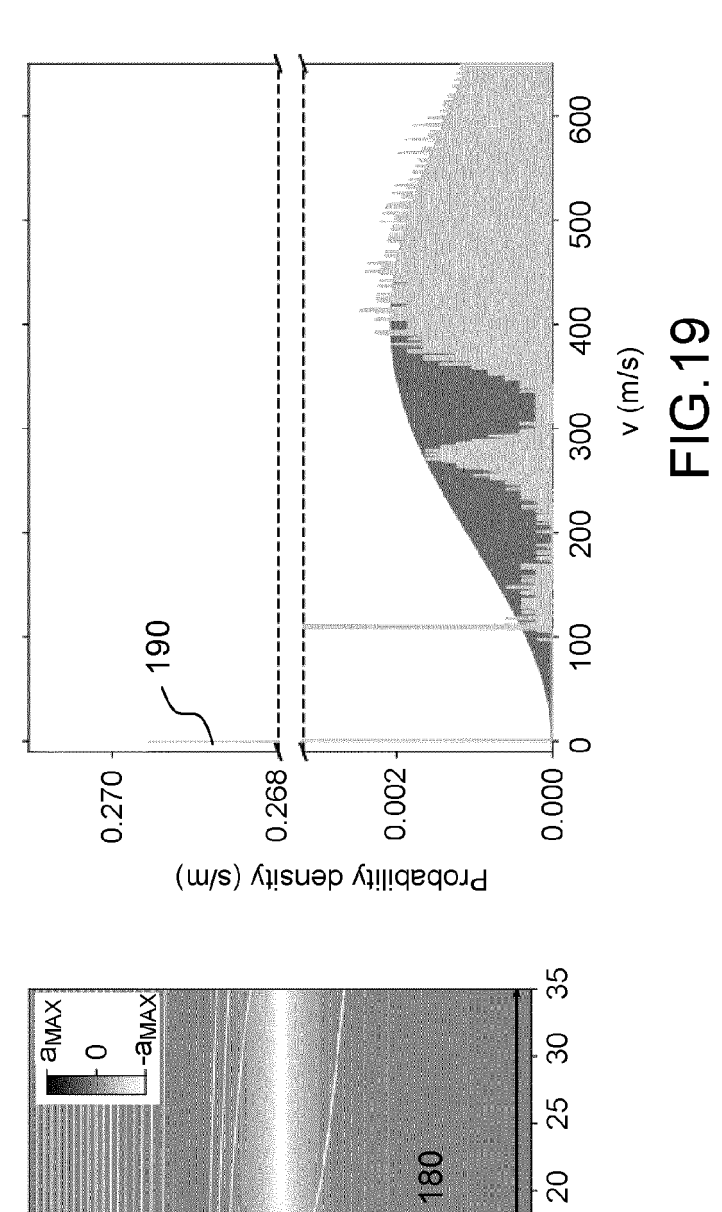


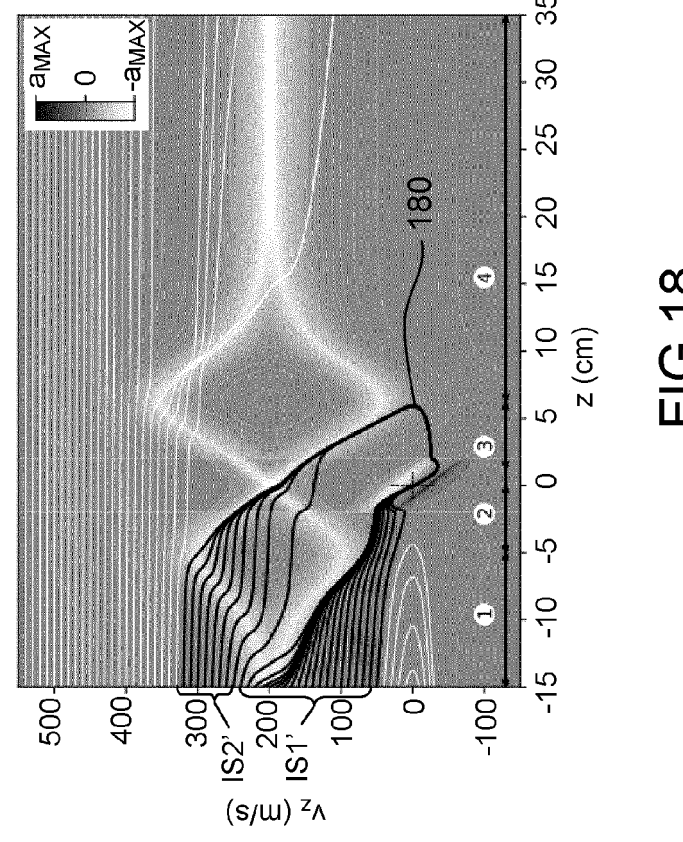


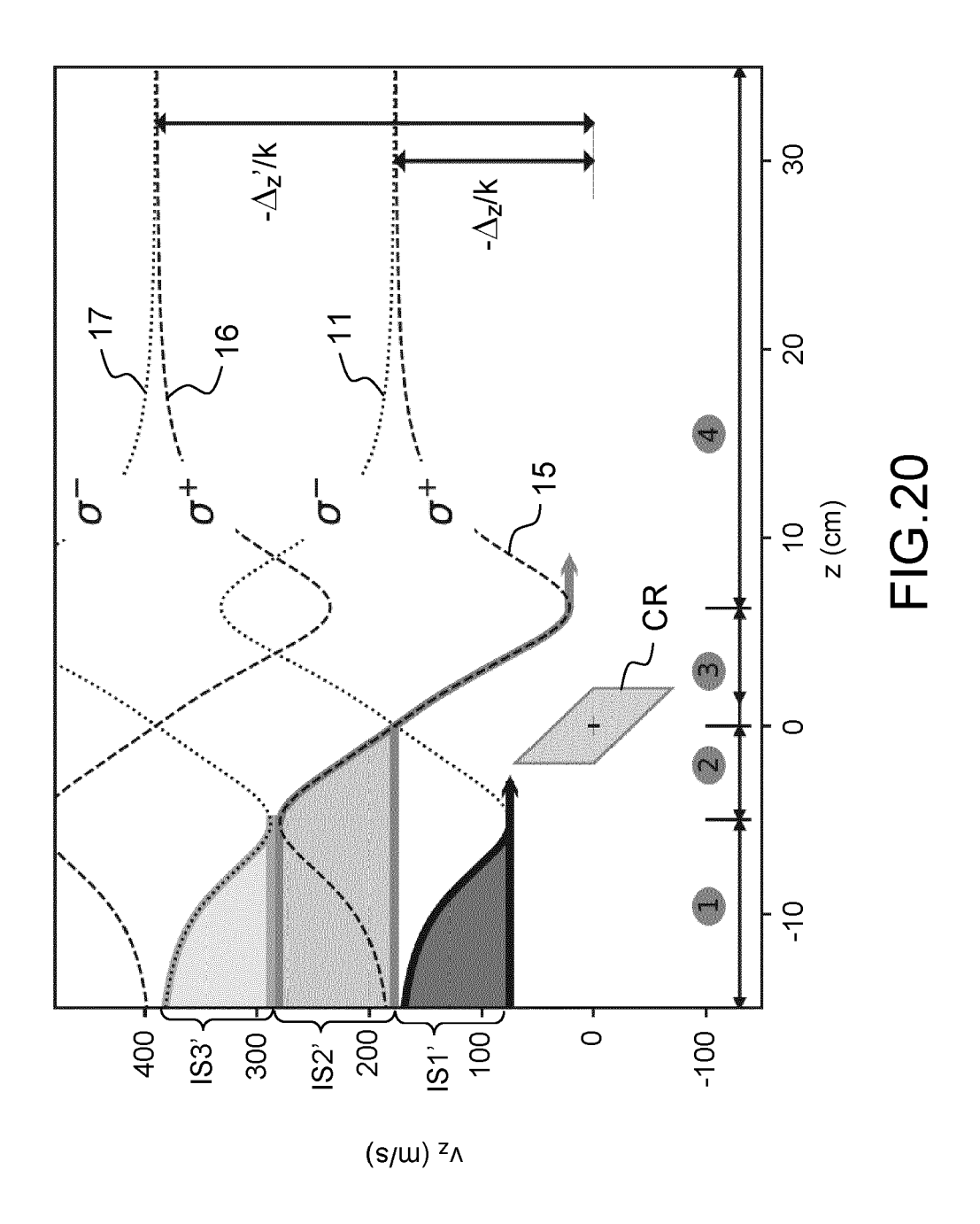


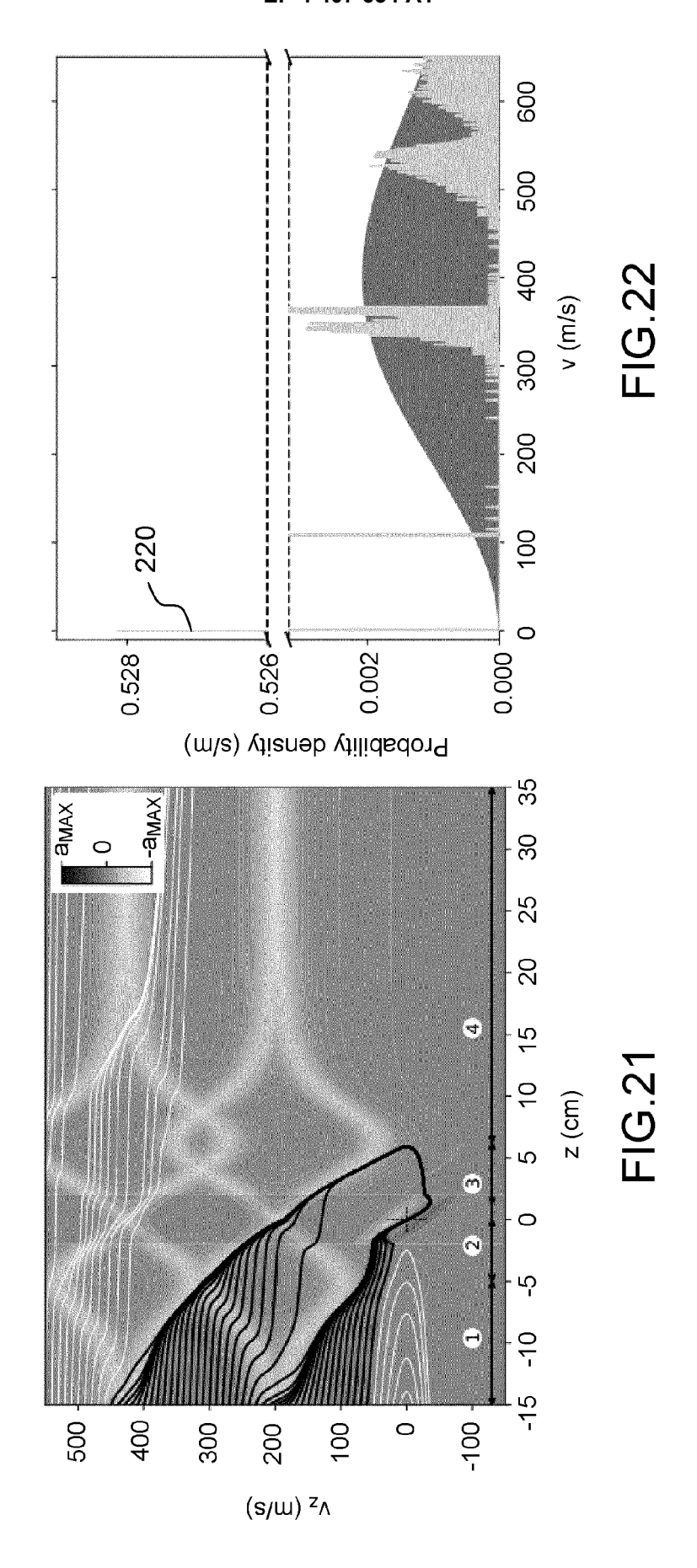
™ B













EUROPEAN SEARCH REPORT

Application Number

EP 23 30 5107

	DOCUMENTS CONSIDERED					
Category	Citation of document with indicatio of relevant passages	n, where appropriate,	Relevant to claim	CLASSIFICATION OF THE APPLICATION (IPC)		
x	JIANING LI ET AL: "Bi-	color atomic beam	1-4,6,	INV.		
	slower and magnetic fie			G21K1/00		
	ultracold gases",	•				
	ARXIV.ORG, CORNELL UNIV	ERSITY LIBRARY, 201				
	OLIN LIBRARY CORNELL UN	IVERSITY ITHACA, NY				
	14853,					
	6 January 2023 (2023-01	-06), XP091408767,				
	DOI: 10.1116/5.0126745					
Y -	* pages 1-5 *		11			
A			5,7			
A,D	INGO NOSSKE ET AL: "Two	 o-dimensional	1			
, -	magneto-optical trap as		_			
	strontium atoms",	· · · · · · · · · · · · · · · · · · ·				
	ARXIV.ORG, CORNELL UNIV	ERSITY LIBRARY, 201				
	OLIN LIBRARY CORNELL UN	IVERSITY ITHACA, NY				
	14853,					
	4 September 2017 (2017-	09-04),				
	XP081282861,	7 020001				
	DOI: 10.1103/PHYSREVA.9° * the whole document *	1.039901		TECHNICAL FIELDS		
				SEARCHED (IPC)		
Y	WO 2015/145136 A2 (UNIV	BIRMINGHAM [GB])	11	G21K		
	1 October 2015 (2015-10-					
	* pages 1-4 *					
_			_			
A	JAROM S JACKSON ET AL: Trap Field Characteriza	-	4			
	Directional Hanle Effect					
	ARXIV.ORG, CORNELL UNIV	•				
	OLIN LIBRARY CORNELL UN					
	14853,					
	10 March 2017 (2017-03-					
	* Methods;					
	figure 1 *					
		 -/				
		-/ 				
	The present search report has been dr	<u> </u>				
	Place of search	Date of completion of the search		Examiner		
	Munich	8 September 2023	Gio	ovanardi, Chiara		
С	ATEGORY OF CITED DOCUMENTS	T : theory or principle	underlying the	invention		
X : part	icularly relevant if taken alone	E : earlier patent doc after the filing date	е			
doci	icularly relevant if combined with another ument of the same category	D : document cited in L : document cited fo	n the application or other reasons			
A : technological background O : non-written disclosure			ee same patent family, corresponding			
() · non	-written disclosure	X · member of the ca	ime patent tamil	v. corresponding		

page 1 of 2



EUROPEAN SEARCH REPORT

Application Number

EP 23 30 5107

Category	Citation of document with indication of relevant passages	on, where appropriate,	Relevant to claim	CLASSIFICATION OF THE APPLICATION (IPC)
_		1 1	_	
A	XIAOBIN MA ET AL: "A o	-	5	
	magneto-optical trap fo	or lithium and		
	strontium atoms",			
	ARXIV.ORG, CORNELL UNIX			
	OLIN LIBRARY CORNELL UN	NIVERSITY ITHACA, NY		
	14853,	10) VD001167611		
	10 April 2019 (2019-04- * the whole document *	-10), XPU8116/611,		
A	GARWOOD DAVIS ET AL: '	'A hybrid Zeeman	5	
	slower for lithium",			
	REVIEW OF SCIENTIFIC IN	STRUMENTS, AMERICAN		
	INSTITUTE OF PHYSICS, 2			
	QUADRANGLE, MELVILLE, N			
	vol. 93, no. 3, 10 Marc	· ·		
	, XP012264115,	•		
	ISSN: 0034-6748, DOI: 1	10.1063/5.0081080		
	[retrieved on 2022-03-1	10]		
	* figure 1 *			
A	KOELEMEIJ J C J ET AL:		7	TECHNICAL FIELDS SEARCHED (IPC)
	trap for metastable hel	lium at 389 nm",		
	ARXIV.ORG, CORNELL UNIV	·		
	OLIN LIBRARY CORNELL UN	·		
	OLIN LIBRARY CORNELL UN 14853,	NIVERSITY ITHACA, NY		
	OLIN LIBRARY CORNELL UN 14853, 15 October 2002 (2002-1	NIVERSITY ITHACA, NY 10-15), XP080096307,		
	OLIN LIBRARY CORNELL UN 14853, 15 October 2002 (2002-1 DOI: 10.1103/PHYSREVA.6	NIVERSITY ITHACA, NY 10-15), XP080096307,		
	OLIN LIBRARY CORNELL UN 14853, 15 October 2002 (2002-1	NIVERSITY ITHACA, NY 10-15), XP080096307,		
	OLIN LIBRARY CORNELL UN 14853, 15 October 2002 (2002-1 DOI: 10.1103/PHYSREVA.6	NIVERSITY ITHACA, NY 10-15), XP080096307,		
	OLIN LIBRARY CORNELL UN 14853, 15 October 2002 (2002-1 DOI: 10.1103/PHYSREVA.6	NIVERSITY ITHACA, NY 10-15), XP080096307,		
	OLIN LIBRARY CORNELL UN 14853, 15 October 2002 (2002-1 DOI: 10.1103/PHYSREVA.6	NIVERSITY ITHACA, NY 10-15), XP080096307,		
	OLIN LIBRARY CORNELL UN 14853, 15 October 2002 (2002-1 DOI: 10.1103/PHYSREVA.6	NIVERSITY ITHACA, NY 10-15), XP080096307,		
	OLIN LIBRARY CORNELL UN 14853, 15 October 2002 (2002-1 DOI: 10.1103/PHYSREVA.6	NIVERSITY ITHACA, NY 10-15), XP080096307,		
	OLIN LIBRARY CORNELL UN 14853, 15 October 2002 (2002-1 DOI: 10.1103/PHYSREVA.6	NIVERSITY ITHACA, NY 10-15), XP080096307,		
	OLIN LIBRARY CORNELL UN 14853, 15 October 2002 (2002-1 DOI: 10.1103/PHYSREVA.6	NIVERSITY ITHACA, NY 10-15), XP080096307,		
	OLIN LIBRARY CORNELL UN 14853, 15 October 2002 (2002-1 DOI: 10.1103/PHYSREVA.6	NIVERSITY ITHACA, NY 10-15), XP080096307,		
	OLIN LIBRARY CORNELL UN 14853, 15 October 2002 (2002-1 DOI: 10.1103/PHYSREVA.6	NIVERSITY ITHACA, NY 10-15), XP080096307,		
	OLIN LIBRARY CORNELL UN 14853, 15 October 2002 (2002-1 DOI: 10.1103/PHYSREVA.6	NIVERSITY ITHACA, NY 10-15), XP080096307,		
	OLIN LIBRARY CORNELL UN 14853, 15 October 2002 (2002-1 DOI: 10.1103/PHYSREVA.6	NIVERSITY ITHACA, NY 10-15), XP080096307,		
	OLIN LIBRARY CORNELL UN 14853, 15 October 2002 (2002-1 DOI: 10.1103/PHYSREVA.6	NIVERSITY ITHACA, NY 10-15), XP080096307,		
	OLIN LIBRARY CORNELL UN 14853, 15 October 2002 (2002-1 DOI: 10.1103/PHYSREVA.6	NIVERSITY ITHACA, NY 10-15), XP080096307, 57.053406		
	OLIN LIBRARY CORNELL UN 14853, 15 October 2002 (2002-1 DOI: 10.1103/PHYSREVA.6 * pages 2-4 *	NIVERSITY ITHACA, NY 10-15), XP080096307, 57.053406		Examiner
	OLIN LIBRARY CORNELL UN 14853, 15 October 2002 (2002-1 DOI: 10.1103/PHYSREVA.6 * pages 2-4 *	IVERSITY ITHACA, NY 10-15), XP080096307, 57.053406	Gio	Examiner
	OLIN LIBRARY CORNELL UN 14853, 15 October 2002 (2002-1 DOI: 10.1103/PHYSREVA.6 * pages 2-4 * The present search report has been of Place of search Munich	irawn up for all claims Date of completion of the search 8 September 2023 T: theory or principle	underlying the i	vanardi, Chiara
	OLIN LIBRARY CORNELL UN 14853, 15 October 2002 (2002-1 DOI: 10.1103/PHYSREVA.6 * pages 2-4 * The present search report has been of Place of search Munich ATEGORY OF CITED DOCUMENTS	drawn up for all claims Date of completion of the search 8 September 2023 T: theory or principle E: earlier patent docu	underlying the i	vanardi, Chiara
X : par Y : par	OLIN LIBRARY CORNELL UN 14853, 15 October 2002 (2002–1 DOI: 10.1103/PHYSREVA.6 * pages 2–4 * The present search report has been of Place of search Munich ATEGORY OF CITED DOCUMENTS ticularly relevant if taken alone ticularly relevant if combined with another	trawn up for all claims Date of completion of the search 8 September 2023 T: theory or principle E: earlier patent doou after the filling date D: document cited in it	underlying the i iment, but publi the application	vanardi, Chiara
X : pari Y : pari doc	OLIN LIBRARY CORNELL UN 14853, 15 October 2002 (2002–1 DOI: 10.1103/PHYSREVA.6 * pages 2–4 * The present search report has been of Place of search Munich ATEGORY OF CITED DOCUMENTS ticularly relevant if taken alone	irawn up for all claims Date of completion of the search 8 September 2023 T: theory or principle E: earlier patent docu after the filing date D: document cited in L: document cited in	underlying the iment, but publi the application other reasons	vanardi, Chiara

page 2 of 2



Application Number

EP 23 30 5107

	CLAIMS INCURRING FEES
	The present European patent application comprised at the time of filing claims for which payment was due.
10	Only part of the claims have been paid within the prescribed time limit. The present European search report has been drawn up for those claims for which no payment was due and for those claims for which claims fees have been paid, namely claim(s):
15	No claims fees have been paid within the prescribed time limit. The present European search report has been drawn up for those claims for which no payment was due.
20	LACK OF UNITY OF INVENTION
	The Search Division considers that the present European patent application does not comply with the requirements of unity of invention and relates to several inventions or groups of inventions, namely:
25	
	see sheet B
30	
	All further search fees have been paid within the fixed time limit. The present European search report has been drawn up for all claims.
35	As all searchable claims could be searched without effort justifying an additional fee, the Search Division did not invite payment of any additional fee.
40	Only part of the further search fees have been paid within the fixed time limit. The present European search report has been drawn up for those parts of the European patent application which relate to the inventions in respect of which search fees have been paid, namely claims:
15	None of the further search fees have been paid within the fixed time limit. The present European search report has been drawn up for those parts of the European patent application which relate to the invention first mentioned in the claims, namely claims:
50	mat menuoned in the dams, namely dams.
55	The present supplementary European search report has been drawn up for those parts of the European patent application which relate to the invention first mentioned in the claims (Rule 164 (1) EPC).



LACK OF UNITY OF INVENTION SHEET B

Application Number

EP 23 30 5107

5

10

15

20

25

30

35

40

45

50

The Search Division considers that the present European patent application does not comply with the requirements of unity of invention and relates to several inventions or groups of inventions, namely:

1. claims: 1-3, 10, 11

Cold atom source comprising :

- a primary atom source (PAS) configured to generate an atomic beam (AtB) propagating along a z direction of a coordinate system xyz,
- a two-dimensional magneto-optical trap, called ${\tt 2D-MOT}$, comprising :
- a first pair (LB1, LB1') and a second pair (LB2, LB2') of two counterpropagating beams, the two pairs being perpendicular to each other and located in a plane yz, the intersection of which defining a trap zone (ZTr) having a centre O,
- a magnetic device (MD) configured to generate a magnetic field having :
- a null value at centre O and on the $\mathbf x$ axis at least inside the trap zone,
- a component along y By having a gradient along the z axis being almost constant in the trap zone, an absolute value of said constant depending on the atom species,
- the component along y By varying along the z axis between two extrema, a positive maximum and a negative minimum, said positive maximum and said negative minimum having identical absolute values,
- a cooling beam (CBm) propagating in a direction opposite to that of the atoms, the cooling beam presenting a frequency detuning with respect to a frequency of a cooling transition having a negative value depending on the atom species, said frequency detuning being determined so that a first set of atoms presenting speeds comprised in a first speed interval (IS1) at an exit of the atom primary source and a second set of atoms presenting speeds comprised in a second speed interval (IS2) greater than the speeds of the first interval, are decelerated by resonance with respectively a first and a second circular polarization component of the cooling beam, the second speed interval (IS2) being contiguous to the first speed interval (IS1).

2. claims: 4-9

Cold atom source comprising:— a primary atom source (PAS) configured to generate an atomic beam (AtB) propagating along a z direction of a coordinate system xyz,— a two-dimensional magneto-optical trap, called 2D-MOT, comprising: a first pair (LB1, LB1') and a second pair (LB2, LB2') of two counterpropagating beams, the two pairs being perpendicular to each other and located in a plane yz, the intersection of which defining a trap zone (ZTr) having a centre O, a magnetic device (MD) configured to generate a magnetic field having a null value at centre O and on the x

55

page 1 of 2



LACK OF UNITY OF INVENTION SHEET B

Application Number

EP 23 30 5107

The Search Division considers that the present European patent application does not comply with the requirements of unity of invention and relates to several inventions or groups of inventions, namely:

axis at least inside the trap zone, a component along y By having a gradient along the z axis being constant in the trap zone, an absolute value of said constant depending on the atom species, the component along y By varying along the z axis between two extrema, a positive maximum and a negative minimum, an absolute value of the extremum located on a side opposite to the primary atom source being strictly greater than an absolute value of the other extremum,— a cooling beam (CBm) propagating in a direction opposite to that of the atoms, the cooling beam presenting a frequency detuning with respect to a frequency of a cooling transition having a negative value depending on the atom species.

page 2 of 2

ANNEX TO THE EUROPEAN SEARCH REPORT ON EUROPEAN PATENT APPLICATION NO.

EP 23 30 5107

5

This annex lists the patent family members relating to the patent documents cited in the above-mentioned European search report. The members are as contained in the European Patent Office EDP file on The European Patent Office is in no way liable for these particulars which are merely given for the purpose of information.

08-09-2023

10	Patent document cited in search report	Publication date	Patent family member(s)	Publication date
	WO 2015145136 Z	A2 01-10-2015	AU 2015237963 A1	03-11-2016
			CN 106664789 A	10-05-2017
45			EP 3123253 A2	01-02-2017
15			JP 6824741 B2	03-02-2021
			JP 2017512639 A	25-05-2017
			US 2017105276 A1	13-04-2017
			WO 2015145136 A2	01-10-2015
20				
20				
25				
30				
35				
40				
40				
45				
50				
	on l			
	FORM P0459			
	프			
55	P			

For more details about this annex : see Official Journal of the European Patent Office, No. 12/82

REFERENCES CITED IN THE DESCRIPTION

This list of references cited by the applicant is for the reader's convenience only. It does not form part of the European patent document. Even though great care has been taken in compiling the references, errors or omissions cannot be excluded and the EPO disclaims all liability in this regard.

Non-patent literature cited in the description

- PHILLIPS et al. Laser Deceleration of an Atomic Beam. *Phys.Rev. Lett.*, 1982, vol. 48 (9 [0003]
- TIECKE et al. High flux two-dimensional magneto-optical-trap source for cold lithium atoms. *Phys. Rev. A*, 2009, vol. 80, 013409 [0015]
- RAAB et al. Phys.Rev. Lett., 1987, vol. 59 (23), 2631 [0023]
- LAMPORESI et al. Review of scientific Instruments, 2013, vol. 84, 063102 [0029]
- NOSSKE et al. Physical. Review A, 2017, vol. 96, 053415 [0029]
- KOCK et al. Laser controlled atom source for optical clocks. *Scientific Reports*, 2016, vol. 6, 37321 [0063]
- GREENLAND et al. Atomic beam velocity distributions. Journal of Physics D: Applied Physics, 1985, vol. 18, 1223 [0089]